ELSEVIER

Prog. Polym. Sci. 27 (2002) 39–85

PROGRESS IN POLYMER SCIENCE

www.elsevier.com/locate/ppolysci

Synthesis of functional polyolefin copolymers with graft and block structures

T.C. Chung*

Department of Materials Science and Engineering, The Pennsylvania State University, University Park, PA 16802, USA

Received 14 July 2001; accepted 31 August 2001

Abstract

This paper reviews a very useful approach in the preparation of polyolefin graft and block copolymers, containing both polyolefin block (PE, PP, *s*-PS, EP, etc.) and functional polymer block (acrylic and methacrylate polymers), with good control of molecular structure. The chemistry involves polyolefin 'intermediates' containing reactive borane, *p*-methylstyrene, and divinylbenzene units in the side chains or at the chain end, which are prepared by the combination of metallocene catalysts and reactive comonomers and chain transfer agents. The incorporated borane and *p*-MS groups can be transformed into 'living' radical and anion, respectively, for initiating graft-from polymerization. On the other hand, the incorporated DVB unit resembles to a styrene monomer that can involve the subsequent polymerization reactions. A broad range of polyolefin graft and block copolymers have been prepared, which have high functional (polar) group concentration without compromising the desirable polyolefin properties, such as crystallinity, melting temperature, elasticity, etc. They are very effective interfacial agents to improve compatibility of polyolefin in polymer blends and composites.

Keywords: Functional polyolefin; Borane monomer; *p*-Methylstyrene; Divinylbenzene; Graft copolymer; Block copolymer

Contents

* Tel.: +1-814-863-1394; fax: +1-814-865-2917.
E-mail address: chung@ems.psu.edu (T.C. Chung).

0079-6700/02/$ - see front matter
PII: S0079-6700(01)00038-7

1. Introduction

Polyolefin — including polyethylene (PE), polypropylene (PP), poly(4-methyl-1-pentene), ethylene–propylene elastomer (EPR), and ethylene–propylene–diene rubber (EPDM) — is the most widely used commercial polymer family, with over 53 billion pounds (24 million tons) [1] US annual production (about 40% worldwide) in 1999, or close to 60% of the total polymer produced. They are greatly influencing our day-to-day life, and range from common items like bread and garbage bags, milk jugs, bottles, containers, hoses, outdoor-indoor carpets, tires, bumpers and trims to bullet-proof jackets. The excellent combination of chemical and physical properties [2–4] along with low cost, superior processability and recyclability has positioned itself as the most preferred choice among commercial polymers.

Despite the great successes, there are some inherent shortfalls in polyolefin materials that prevent their even wider usage in many areas currently occupied by other polymers that are much more expensive and less environmentally friendly materials. The major stumbling block has been the poor adhesion and incompatibility between polyolefin and other materials, such as pigments, glass fibers, clays, metals, carbon black, fillers and most polymers. Due to lack of chemical functionality (polar groups) and semi-crystalline morphology (in PE, PP, etc.), polyolefin naturally exhibits low surface energy. For examples, polyolefin is most commonly used for films and molded articles where single polyolefin is required, and it is inadequate for polymer blends and composites, those in which adhesion and compatibility with other materials is paramount.

Since the discovery of HDPE and PP about a half century ago, functionalization of polyolefin has been a scientifically challenging and industrially important area [5–8]. The constant interest, despite the lack of effective functionalization chemistry, is obviously due to the strong desire to improve polyolefin's poor interactive properties and broaden polyolefin applications to higher value products, especially in polymer blend and composite areas. With the recent decade of fierce worldwide competition in single site transition metal (metallocene and non-metallocene) coordination catalysis [9–15], defined polymerization mechanisms, many research activities were geared toward the preparation of functional polyolefin copolymers.

2. General functionalization approaches

Theoretically, there are three possible approaches to the functionalization of polyolefin, as illustrated in Scheme 1. They include (a) direct copolymerization of α-olefin with functional monomer, (b) chemical modification of the preformed polymer, and (c) reactive copolymer approach by incorporating reactive comonomers that can be selectively and effectively interconverted to functional groups.

The first two approaches are more obvious and naturally have enjoyed the most attention. In the past, they were referred to as direct and post-polymerization processes, respectively. The direct process could be an ideal one (one-step reaction) if the copolymerization reaction with functional monomers would be as effective and straightforward as the corresponding homopolymerization reaction. Unfortunately, some fundamental chemical difficulties, namely catalyst poisoning and other side reactions, have prevented serious consideration of the direct process for commercial application. The Lewis acid components (Ti, Zr, Hf, V and Al) of the catalyst will tend to complex with non-bonded electron pairs on N, O, and X (halides) of functional monomers in preference to react with the π-electrons of the double bonds. The net result is the deactivation of the active polymerization sites by formation of stable complexes between catalysts and functional groups, thus inhibiting polymerization.

So far, most research activities in this direct process have been focused on the prevention of catalyst poison by (i) protecting sensitive functional group from poisoning catalyst [16–20], or (ii) employing catalysts that are less oxophilic and more stable to heteroatoms [14,15,21]. In general, both methods have their own concerns and limitations. Some protected functional groups, via acid-base complexization, reduces the solubility of the propagating polymer chain, which in turn reduces catalyst efficiency. On the other hand, in steric protection cases it is very important to choose the bulky protecting group that can not only prevent catalyst poisoning, but also can be effectively deprotected. However, the expensive protection and deprotection reactions, with some environmental concerns due to by-products, prohibit any large-scale commercialization.

In recent years, some very interesting results were reported by using less oxophilic late transition metal catalysts, such as Fe, Ni, Co and Pd complexes, in the copolymerization of α-olefins and acrylate monomers. The combination of a less oxophilic catalyst and an electronic-protected functional group significantly increases catalyst activity, indicating that the lone pair electrons in the heteroatom (such as

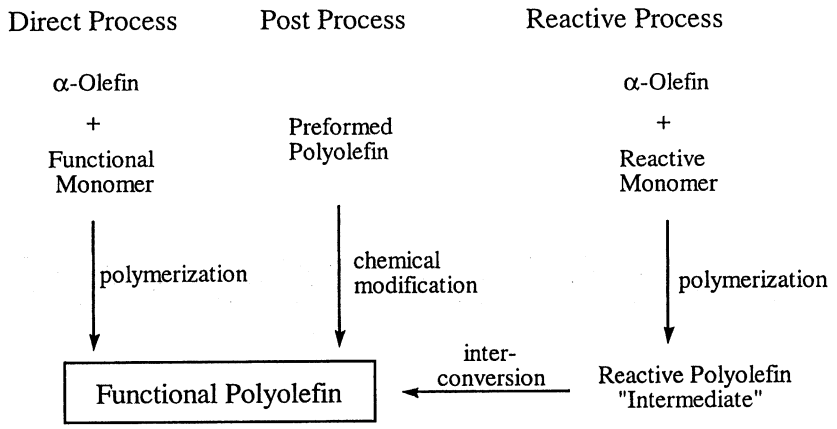

Scheme 1.

O and N) still compete with the olefin insertion during the late transition metal polymerization [21]. The polymer produced usually contains a branched molecular structure with relatively low (or no) melting temperature and crystallinity. There is no example of steric-specific polymerization of α-olefin by using late transition metal catalysts. It is very challenging to prepare functionalized *i*-PP or *s*-PS polymers by this route.

Currently, most of the commercial functionalization processes are based on post-polymerization process [22–26]. Chemical modification of the pre-formed polyolefin homopolymers has been usually carried out in situ during the fabrication process to reduce the production cost, as well as to relieve the significant concern (in many cases) of reducing processibility of polyolefin after functionalization reaction. However, the combination of the inert nature of polyolefin (requiring highly energetic reaction conditions) and a very short reaction time (during the processing) causes a great deal of difficulties in controlling polymer composition and structure. There is no facile reaction site in the saturated PE, PP and EP polymers. The only way is to activate the polymer by breaking some stable C–H bonds and forming free radicals along the polymer chain. The resulting polymeric radicals then undertake chemical reactions with some chemical reagents, such as maleic anhydride. However, this functionalization reaction is usually accompanied with many undesirable side reactions (crosslinking and degradation) and by-products. Overall, the current commercial process is far from the ideal one.

The third functionalization approach is a relatively new one (mostly developed in our laboratory) [27–32]. The basic idea is to circumvent the chemical difficulties in both direct and post-polymerization processes by designing a reactive copolymer 'intermediate' that can be effectively synthesized and subsequently interconverted to functional polymer. This approach has benefited greatly from metallocene technology, especially due to its superior capability in the copolymerization and chain transfer reactions. As will be discussed later, several new reactive comonomers can be effectively incorporated into polyolefins in the side chains or at the chain end. In turn, these reactive groups incorporated in polymer open up a lot of possibility to produce new polyolefin products, including functional graft and block copolymers, that would be very difficult to prepare by other methods.

3. Functional polyolefins with graft and block structures

One of the major concerns in the functionalization of polyolefin (PE or PP) is the alternation of some desirable polyolefin properties, such as melting temperature, crystallinity, etc. which are essential for an effective compatibilizer in polymer blends and composites. However, the introduction of high concentration of functional groups along the polymer chain (such as PE and PP) will inevitably reduce its crystallinity and melting temperature, as well as its co-crystallization ability with pure PE or PP polymer (in matrix).

Functional polyolefin with block and graft structures (illustrated in Scheme 2) are the most desirable material, which not only offer large quantity of functional groups, but also preserve the original polyolefin properties. As the established technique for improving the interfacial interaction, block and graft copolymers are the ideal compatibilizers [33–35] that can dramatically increase the adhesion of polyolefin. In the ideal polyolefin blends and composites, the graft/block copolymers are located at the interfaces, the functional polymer segments provide good adhesion to the polar surfaces, and the polyolefin segments can interpenetrate (with entanglements or/and co-crytallization) into pure polyolefin homopolymer domains.

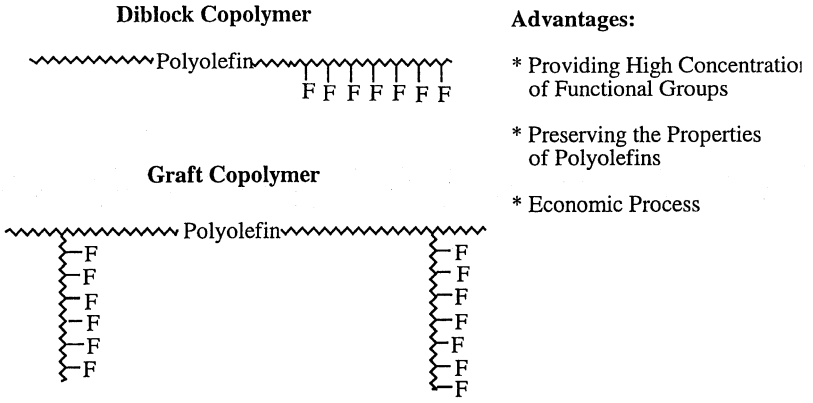

Scheme 2.

In terms of the feasibility of mass-producing polyolefin block and graft copolymers, only a very few linkages (chemical bonds) exist for connecting polymer segments. In other words, the ideal chemical process only requires a few active sites in the polyolefin chain. With the appropriate choice of reactive comonomer or chain transfer agent, it is very possible to produce both block and graft copolymers in an economical fashion.

4. Reactive polyolefin approach

As discussed, both direct and post-polymerization processes have only achieved very limited successes in the functionalization of polyolefins. It is very interesting to explore the alternative routes to prepare functional polyolefins, especially those having block and graft structures. In the past decade, our group has been focusing on a reactive polyolefin approach. As illustrated in Scheme 3, the reactive polyolefin can be prepared by the copolymerization reaction of α-olefin and a selected 'reactive'

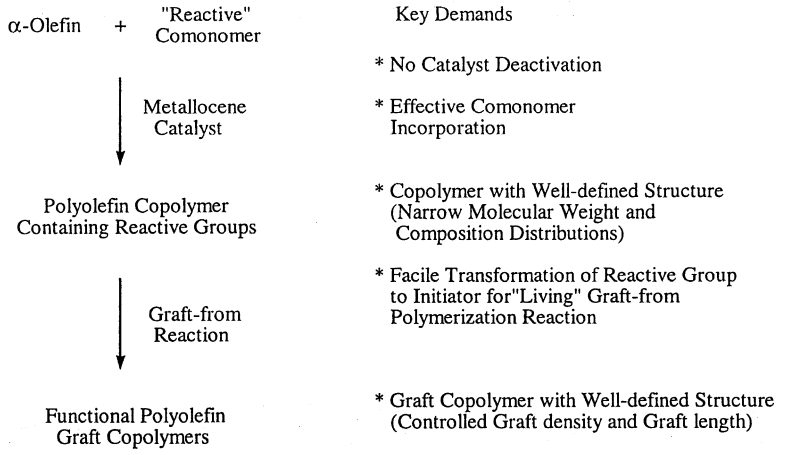

Scheme 3.

comonomer using metallocene catalyst. The formed reactive polyolefin copolymer serves as the intermediate for the preparation of graft copolymers.

Obviously, the key factor in this approach is the design of a comonomer containing a reactive group that can simultaneously fulfill the following requirements. First, the reactive group must be stable to metallocene catalysts and soluble in hydrocarbon polymerization media. Second, the reactive monomer should have good copolymerization reactivity with α-olefins. Third, the reactive group must be facile in the subsequent interconversion reaction to form a stable initiator for the polymerization of functional monomers. In other words, each incorporated reactive group can produce a functional polymer chain containing hundreds of functional groups.

As will be discussed, three reactive comonomers — including borane monomers [36–41], *p*-methylstyrene (*p*-MS) [42–48], and divinylbenzene (DVB) [49] — have been effectively incorporated into polyolefinns with narrow molecular weight and composition distributions.

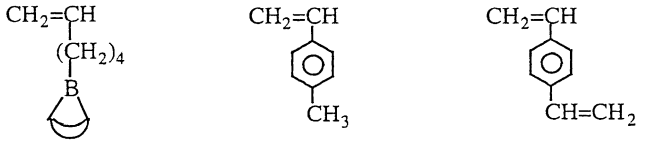

All three reactive sites, i.e. borane, benzylic protons, and styrene units, pending along the polyolefin backbone are very versatile in the subsequent graft reactions. The graft reactions are selectively taken place at the reactive sites, and the concentration of functional groups is basically proportional to the concentration of the reactive sites and functional monomers. As will be discussed later, three reactive comonomers provide complemental coverage of the most desirable functional polyolefin compositions and structures.

It is very interesting to note that the reactive polyolefin approach has also been extended to the preparation of polyolefin containing a reactive terminal group (borane or *p*-methylstyrene) and polyolefin diblock copolymers [50–52]. One example is illustrated in Scheme 4.

As will be discussed, the combination of chain transfer and hydroboration reactions provides a convenient route to prepare a broad range of polyolefins containing a reactive terminal group, which include all commercial polyolefins (PE, PP, *s*-PS, and their *co*- and *ter*-polymers). In turn, the terminal reactive group (borane or *p*-methylstyrene) can be transformed to living free radical or anionic initiator, respectively, for chain extension reaction to form diblock copolymers. The overall reaction process resembles a transformation from metallocene polymerization to living free radical polymerization via a borane terminal group or to living anionic polymerization via a *p*-methylstyrene terminal group.

5. Synthesis of polyolefin containing reactive groups

5.1. Polyolefins containing borane side groups

Copolymerization of α-olefin and borane monomer (a high α-olefin containing a borane moiety) is a very convenient way to prepare borane-containing polyolefin. Due the unique features of borane moiety, including good stability to metallocene catalyst and good solubility [8] in organic solvents used in the polymerization, borane monomer generally behaves similarly to the corresponding high α-olefin. In other words, we could treat the borane monomer as a high α-olefin in the copolymerization reaction and expect similar copolymer structure that is governed by the reactivity ratios of two comonomers under

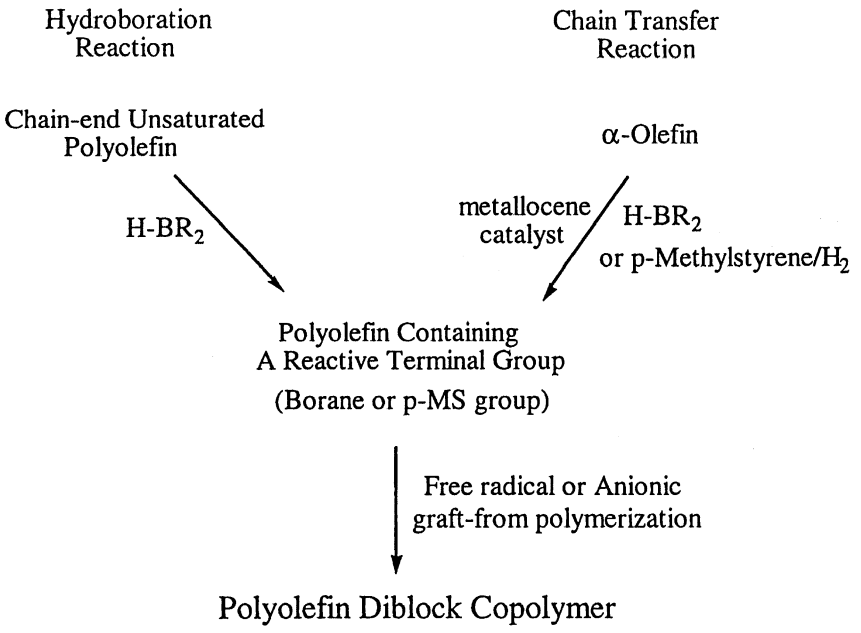

Scheme 4.

each set of the catalyst system. In the Ziegler–Natta heterogeneous catalyst system, the reactivity of monomer is dramatically dependent on the size of the monomer — the bigger the size of the monomer, the lower the reactivity. Ethylene is generally five times more reactive than propylene, and the reactivity becomes more constant in high α-olefins. It could be predicted that the copolymerization of ethylene with borane monomer would be very difficult in Ziegler–Natta heterogeneous catalyst system [39]. The borane monomer may have a better chance to be incorporated with propylene [40,41] and high α-olefins, such as 1-butene and 1-octene [38]. On the other hand, the use of a homogeneous metallocene catalyst with constrained ligand geometry (having an open active site) could significantly improve the copolymerization ability of borane monomers with ethylene.

The copolymerization reaction between ethylene and 5-hexenyl-9-BBN [39] is the best testing ground for studying the copolymerization ability of borane monomer, especially in terms of its dependence on the Ziegler–Natta and metallocene catalysts. Eq. (1) shows the copolymerization of ethylene and a borane monomer, such as 5-hexenyl-9-BBN, by various catalyst systems. The reactions were carried out in a Parr reactor under N_2 atmosphere.

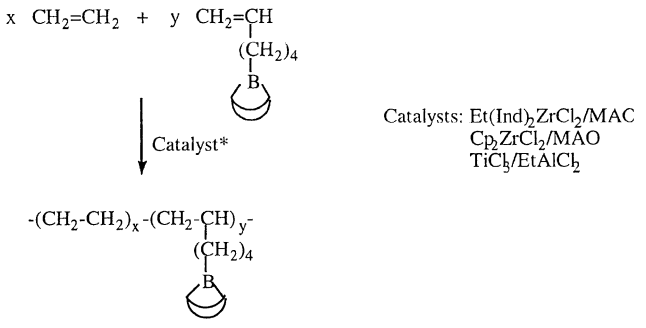

(1)

Table 1
A summary of copolymerization reactions between ethylene (m_1) and 5-Hexenyl-9-BBN (m_2)

Run number	Catalyst type[a]	Comonomers m_1/m_2 (psi)[b]/(g)	Reaction temperature/time (°C/min)	Catalyst activity (Kg/mol hr)	Borane in copolymer (mol%)
A-1	I	45/0	30/60	644	0
A-2	I	45/0.56	30/30	1469	1.25
A-3	I	45/1.52	30/30	2020	2.15
A-4	I	45/2.10	30/30	2602	2.30
B-1	II	45/0	30/70	337	0
B-2	II	45/5	30/70	643	1.22
C-1	III	80/10	60/110	4.0	0

[a] Catalysts: $Et(Ind)_2ZrCl_2$/MAO (I), Cp_2ZrCl_2/MAO (II) and $TiCl_3$·AA/Et_2AlCl (III), solvent: 100 ml toluene.
[b] Corresponding to 0.38 mol/l.

Three catalyst systems, including two homogeneous metallocene $Et(Ind)_2ZrCl_2$ and Cp_2ZrCl_2 with MAO catalysts and one heterogeneous $TiCl_3$·AA/$(Et)_2AlCl$ catalyst, were evaluated in the copolymerization reactions. Usually, the reaction was initiated by charging the catalyst solution into the mixture of ethylene and 5-hexenyl-9-BBN, and a constant ethylene pressure was maintained throughout the polymerization process. Almost immediately, white precipitate was observed at the beginning of the reaction. After a specific reaction time, the copolymerization was terminated by addition of IPA.

Table 1 summarizes the experimental results. Overall, the homogeneous metallocene catalysts, especially $Et(Ind)_2ZrCl_2$/MAO with stained ligand geometry and an open active site, show satisfactory copolymerization results at ambient temperature. Comparing runs A-1–A-4, the concentration of borane groups in PE is basically proportional to the concentration of borane monomer feed. About 50–60% of borane monomers was incorporated into the PE copolymers after about a half hour. It was very unexpected that the catalyst activity systematically increased with the concentration of borane monomer in the $Et(Ind)_2ZrCl_2$/MAO catalyst system. Obviously, no retardation due to the borane groups is shown in these cases. The copolymerization of borane monomers in Cp_2ZrCl_2/MAO system (shown in run B-2) is significantly more difficult — only 1.22 mol% of borane monomer incorporated in PE copolymer even high concentration of borane monomer used. On the other hand, the heterogeneous $TiCl_3$·AA/Et_2AlCl catalyst shows no detectable amount of borane group in the copolymer as shown in run C-1.

Fig. 1 shows the GPC curves of poly(ethylene-*co*-5-hexenyl-9-BBN) copolymers containing 0.5 and 1.2 mol% of 5-hexenyl-9-BBN, respectively. Due to the air-sensitivity of the borane group, most of the analyses were carried out on the corresponding hydroxy or ester polymers after converting borane to hydroxy or ester groups. The copolymers were prepared by the $Et(Ind)_2ZrCl_2$/MAO catalyst. Overall, the copolymers have high molecular weight and narrow molecular weight distribution ($M_w/M_n < 3$). There is no indication of any negative influence of borane group on the metallocene polymerization.

This α-olefin/borane monomer copolymerization reaction has been applied to prepare other polyolefin *co*- and *ter*-polymers using metallocene and Ziegler–Natta catalysts. Some semicrystalline copolymers, including poly(ethylene-*co*-B-5-hexenyl-9-BBN), poly(propylene-*co*-B-5-hexenyl-9-BBN) and poly(1-butene-*co*-B-5-hexenyl-9-BBN), were found to contain low concentration of borane monomers (<10 mol%), and are insoluble in common organic solvents at room temperature, but soluble at higher temperatures. However, the copolymers of poly(1-octene-*co*-B-5-hexenyl-9-BBN) (PO-B) and terpolymers

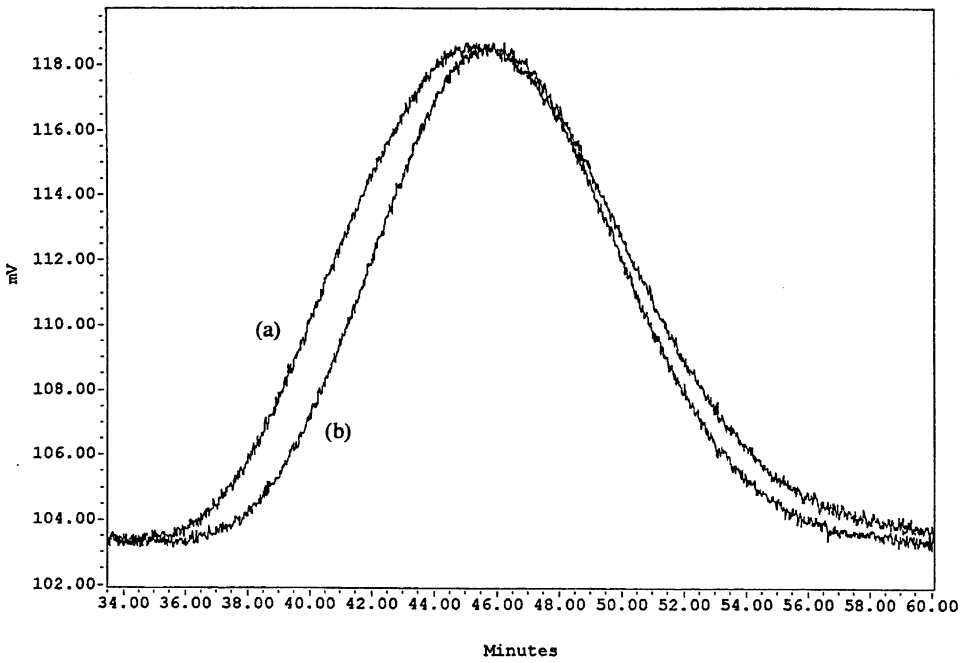

Fig. 1. GPC curves of poly(ethylene-*co*-5-hexenyl-9-BBN) copolymers containing (a) 0.5 and (b) 1.2 mol% of 5-hexenyl-9-BBN.

of poly(ethylene-*ter*-propylene-*ter*-B-5-hexenyl-9-BBN) (EP-B) were found to be soluble in most hydrocarbon solvents at room temperature.

Alternatively, borane-containing polyolefins were prepared by hydroboration of unsaturated polyolefins, such as poly(propylene-*co*-1,4-hexadiene) [53] and poly(ethylene-*co*-propylene-*co*-1,4-hexadiene) [54]. The internal double bond was reacted by dialkylborane, such as 9-BBN. The reaction is very effective in both homogeneous and heterogenious solutions under mild reaction conditions. The concentration of borane groups in polyolefin was controlled by the amount of 9-BBN used in the hydroboration reaction and the concentration of unsaturation in the copolymers. In a typical hydroboration reaction, a THF solution of the borane reagent (e.g. 9-BBN) was added to a toluene suspension of the unsaturated polymer (e.g. inhibitor-free poly(propylene-*co*-1,4-hexadiene) containing 1.7% 1,4-hexadiene units). The suspension was heated to 65°C in a flask equipped with a condenser. After stirring for 5 h, the polymer was precipitated into 150 ml dry/degassed isopropanol and isolated by filtration (in dry-box). The borane-containing polymer was then placed in a suspension of THF for further oxidation reactions.

5.2. Polyolefins containing p-methylstyrene side groups

The second reactive comonomer can be effectively incorporated into polyolefins is *p*-methylstyrene (*p*-MS), which is advantaged by its commercial availability. In general, the preparation of *p*-MS containing polyolefin copolymers has been greatly enhanced by the metallocene catalyst with constrained ligand geometry, having a spatially opened catalytic site, allows the effective incorporation of styrenic

comonomers (Eq. (2)), which was almost impossible by using Ziegler–Natta catalysts:

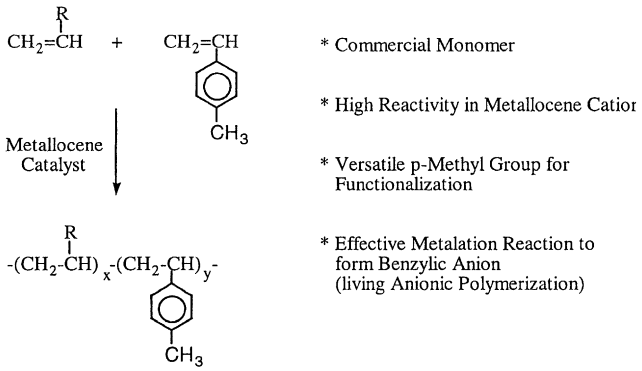

(2)

Table 2 summarizes the results by using three metallocene catalysts, including a simple Cp_2ZrCl_2 catalyst and two bridged $Et(Ind)_2ZrCl_2$ and $[C_5Me_4(SiMe_2N^tBu)]TiCl_2$) catalysts [45,46]. The copolymerization efficiency follows the sequence of $[C_5Me_4(SiMe_2N^tBu)]TiCl_2 > Et(Ind)_2ZrCl_2 > Cp_2ZrCl_2$, which is directly relative to the spatial opening at the active site. In run P-377, about 90% of the *p*-MS was incorporated into the copolymer in 1 hour. In run P-383, the reaction produced copolymer containing 40 mol% of *p*-MS, which is close to the ideal 50 mol% (as known that the consecutive insertion of *p*-MS in all three catalyst systems is almost impossible).

Fig. 2 shows the typical GPC and DSC curves of the homo- and copolymers prepared by the $[C_5Me_4(SiMe_2N^tBu)]TiCl_2$ catalyst. The uniform molecular weight distribution in all samples, with $M_w/M_n = 2$–3, implies the single-site polymerization mechanism. DSC curves show that even a small amount (~1 mol%) of *p*-MS comonomer incorporation has a significant effect on the crystallization of PE. The melting point (T_m) and crystallinity (χ_c) of the copolymer are strongly relative to the density of the comonomer — the higher the density, the lower the T_m and χ_c. Only a single peak is observed throughout the whole composition range, and the melting peak completely disappears at ~10 mol% of *p*-MS concentration.

The copolymerization of propylene and *p*-MS was not effective in producing PP-*p*-MS copolymers [47], completely opposite to those observed in the corresponding ethylene/*p*-MS copolymerization reaction. The drastic differences are due to the steric jamming phenomenon in the cross-over k_{21} reaction (from *p*-MS to propylene), as illustrated in Eq. (3).

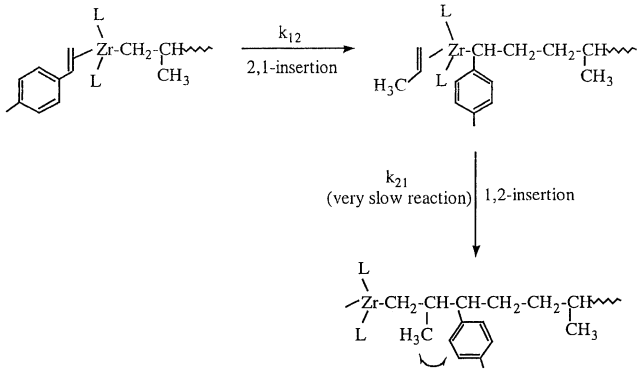

(3)

It is well known that in metallocene catalytic polymerization, the insertion of the styrene monomer is

Table 2
Summary of copolymerization reactions (45 psi ethylene ~0.309 mol/l in toluene, 0.424 mol/l in hexane at 50°C; ~0.398 mol/l in toluene, 0.523 mol/l in hexane at 30°C. 10 psi ethylene ~0.116 mol/l in hexane at 30°C) between Ethylene and *p*-MS

Run number	Catalyst (μmol)[a]	Ethylene/*p*-MS (psi/M)	Solvent/ temperature (°C)	Yield (g)	Catalyst efficiency kg P/mol Mh	*p*-MS in copolymer (mol%)	Conversion of *p*-MS (%)
p-363	I/17	45/0.678	Hexane/50	24.2	1423.5	2.2	26.2
p-365	I/17	45/0.678	Toluene/50	8.44	496.5	1.84	7.7
p-356	II/17	45/0.085	Hexane/50	6.5	382.4	1.83	47.2
p-358	II/17	45/0.678	Hexane/50	21.9	1288.2	5.16	51.1
p-361	II/17	45/1.36	Hexane/50	18.9	1111.8	7.2	29
p-371	II/17	45/2.03	Hexane/50	20.8	1223.5	8.94	25.4
p-357	II/17	45/0.085	Toluene/50	5.7	335.3	1.3	29.9
p-360	II/17	45/0.678	Toluene/50	15.1	888.2	4.76	32.8
p-362	II/17	45/1.36	Toluene/50	19.5	1147.1	6.36	27
p-375	II/17	45/2.03	Toluene/50	19.4	1141.2	8.49	22.8
p-270	III/10	45/0	Toluene/30	4.4	440	-	-
p-377	III/10	45/0.447	Hexane/30	12	1200	13.5	90.3
p-378	III/10	45/0.912	Hexane/30	15.5	1550	22.6	81.3
p-267	III/10	45/0.447	Toluene/30	13	1300	10.9	83.8
p-379	III/10	45/0.912	Toluene/30	17.4	1740	21.6	86.9
p-380	III/10	45/1.82	Toluene/30	24.2	2420	32.8	75.8
p-383	III/10	10/1.82	Hexane/30	15.9	1590	40	54.6

[a] I: Cp_2ZrCl_2/MAO; II: $Et(Ind)_2ZrCl_2$/MAO; III: $[(C_5Me_4)SiMe_2N(t\text{-}Bu)]TiCl_2$/MAO.

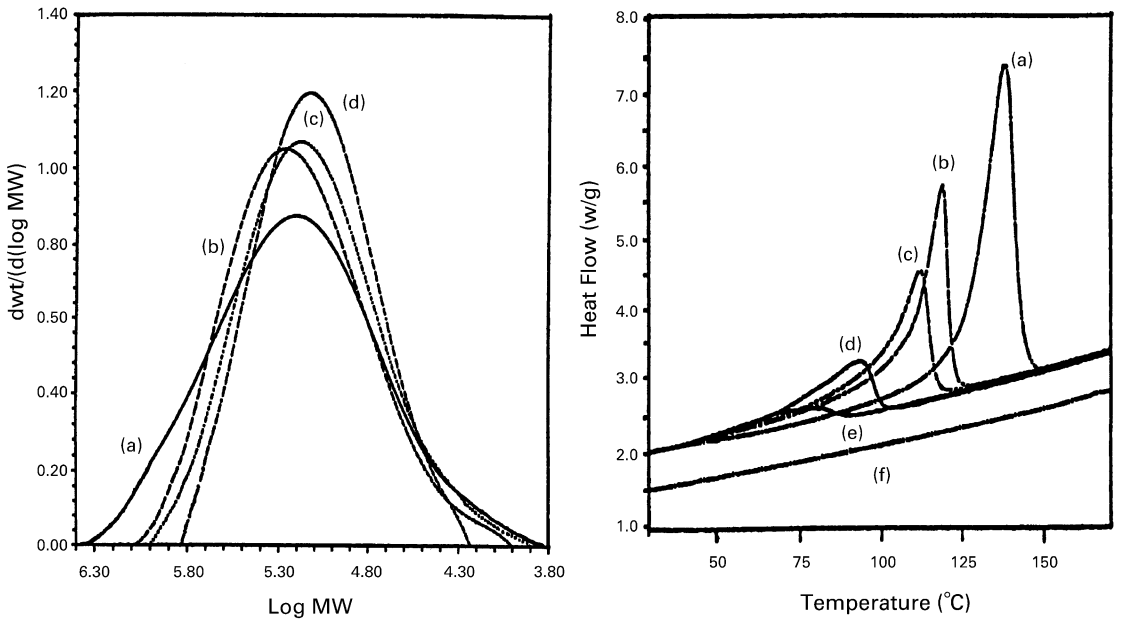

Fig. 2. Left: GPC curves of (a) PE and three PE-*p*-MS copolymers, containing (b) 1.08, (c) 9.82 and (d) 18.98 mol% of *p*-MS units; (right) DSC curves of (a) PE and PE-*p*-MS containing (b) 1.08, (c) 2.11, (d) 5.40, (e) 9.82 and (f) 18.98 mol% of *p*-MS.

predominately secondary (2,1-insertion), while the 1,2-insertion of the propylene monomer is dominant. Once the propagating PP chain has a chance to react with the *p*-MS monomer (k_{12} reaction) via 2,1-insertion, the bulky *p*-phenyl group in the last unit of the growing chain is adjacent to the central metal atom and blocks the upcoming 1,2-insertion of a propylene unit (i.e. k_{21} reaction). Since the homopolymerization (k_{22}) of *p*-MS via the metallocene coordination mechanism is known to be near zero, the metallocene active site at *p*-MS unit dramatically slows the propagation process. Therefore, a small amount of *p*-MS significantly reduces the catalyst reactivity.

Despite the difficulty in propylene/*p*-MS copolymerization, the terpolymerization involving ethylene was very effective, the dormant species shown in Eq. (3) reacts with ethylene to continue the reaction. Tables 3 and 4 summarize the experimental results of the terpolymerization reactions of ethylene/propylene/*p*-MS and ethylene/1-octene/*p*-MS to prepare EP-*p*-MS and EO-*p*-MS terpolymers [48], respectively. Both reactions were carried out by using $[C_5Me_4(SiMe_2N^tBu)]TiCl_2$/MAO catalyst. Overall, the catalyst shows excellent activity in all terpolymerization reactions. The incorporation of *p*-MS seems quiet insensitive to the ethylene/propylene or ethylene/1-octene feed ratios. The molecular weight of terpolymer is quiet high ($M_w \sim 200,000$ g/mol) and is not significantly dependent on the content of *p*-MS. In addition, the molecular weight distributions (M_w/M_n) < 3, similar to most metallocene-based homo- and co-polymers, indicate single-site reaction with good comonomer reactivities

The glass transition temperature (T_g) was examined by DSC. All samples show a well-defined T_g with shape transition, indicating uniform terpolymer structures. The T_g is clearly a function of *p*-MS content. Comparing runs p-116 and p-120, both with ideal ~54 mol% ethylene content and only a very small difference in *p*-MS/propylene mole ratios (0/46 vs. 1.8/44), the T_gs are -50 and -45°C, respectively. Overall, the composition of EP-*p*-MS material with low $T_g < -45$°C is very limited, only to the

Table 3
A summary of Terpolymerization (polymerization conditions: 100 ml toluene; [Ti] = 2.5×10^{-6} mol; [MAO]/[Ti] = 3000; 50°C; 15 min) of ethylene/propylene/*p*-MS by using [$C_5Me_4(SiMe_2N^tBu)$]$TiCl_2$/MAO (Reproduced with permission from Macromolecules 1998;31:2028. Copyright 1998 Am. Chem. Soc.)

Run number	Monomer feed [E]/[P]/[*p*-MS] (mol/l)	Catalyst activity kg/mol Ti h	Copolymer [E]/[P]/[*p*-MS] (mol%)	T_g (°C)	M_w (g/mol)	M_n (g/mol)
p-116	0.13/0.28/0	4.9×10^3	53.9/46.1/0	−49.4	300,400	134,300
p-117	0.12/0.35/0	4.7×10^3	41.8/58.2/0	−43.7	284,300	120,800
p-118	0.12/0.35/0.3	4.0×10^3	46.4/43.6/10.0	−20.7	198,200	74,900
p-119	0.12/0.35/0.05	4.0×10^3	46.1/52.3/1.6	−41.0	195,800	75,100
p-120	0.13/0.28/0.05	4.1×10^3	54.4/43.8/1.8	−45.8	237,700	107,500
p-127	0.13/0.28/0.03	3.8×10^3	50.7/48.6/0.7	−45.9	244,300	85,500
p-128	0.14/0.25/0.03	4.4×10^3	56.3/43.1/0.6	−48.6	269,400	104,300

polymers with <2 mol% of *p*-MS content. Despite the random terpolymer structure and the ideal (~55/45) ethylene/propylene ratio, a further increase of *p*-MS raises the T_g of the terpolymer to > -40°C. On the other hand, the EO-*p*-MS sample with even up to 8 mol% of *p*-MS still shows $T_g < -45$°C, these results clearly show the advantages of the 1-octene comonomer (over propylene), which assures the formation of an amorphous polyolefin elastomer with low T_g and high *p*-MS content.

5.3. Polyolefins containing divinylbenzene side groups

The third reactive comonomer having been incorporated into polyolefin was divinylbenzene (DVB)

Table 4
Summary of terpolymerization (polymerization conditions (unless specified otherwise): 100 ml of toluene; [Ti] = 2.5×10^{-6} mol; [MAO]/Ti = 3000; 50°C; 30 min) of ethylene, 1-octene and *p*-MS using [$C_5Me_4(SiMe_2N^tBu)$]$TiCl_2$/MAO metallocene catalyst [306] (Reproduced with permission from Macromolecules 1998;31:2028. Copyright 1998 Am. Chem. Soc.)

Run number	Monomer concentration in feed (mol/l)			Yield (g)	Copolymer composition (mol%)			T_g (°C)	M_w (g/mol)	M_n (g/mol)	PD
	E[a]	l-Oct	*p*-MS		[*E*]	[O]	[*p*-MS]				
p-470	0.20	0.80	0.10	7.3	54.2	43.0	2.7	−56.2	173,989	74,703	2.3
p-471	0.40	0.80	0.10	10.1	61.1	36.0	2.9	−58.1	219,752	96,802	2.3
p-472	0.40	0.80	0.20	9.8	60.3	36.3	4.4	−55.7	182,185	77,497	2.4
p-473	0.40	0.40	0.20	8.2	59.6	34.0	6.4	−50.1	208,920	86,812	2.4
p-477	0.40	0.20	0.20	6.4	80.2	14.1	5.7	−37.3	227,461	91,490	2.5
p-476	0.40	0.80	0.40	9.0	63.4	29.3	7.3	−50.3	202,085	96,035	2.1
p-475	0.40	0.60	0.40	9.1	67.2	24.7	8.1	−48.2	205,124	93,763	2.2
p-478	0.40	0.40	0.40	7.9	73.3	18.5	8.1	−44.7	246,300	122,306	2.0
p-474	0.40	0.60	0.15	9.0	64.7	31.3	4.0	−55.7	224,476	102,617	2.2

[a] Solubility of ethylene: 0.25 mol/l for 29 psi in hexane at 60°C, 0.20 mol/l for 2 bar, 0.40 mol/l for 4 bar in toluene at 50°C. 0.52 mol/l for 45 psi in hexane at 30°C, 0.13 mol/l for 10 psi in hexane at 30°C.

[49], which results in the polyolefin copolymers with pending styrene units that can serve as the active sites for many graft reactions. The potential problem in the polymerization reaction is the double enchainment of DVB, which will lead to the crosslinked product [55]. In fact, DVB is known as a good crosslinker in many free radical polymerizations. In our laboratory, we have been investigating the metallocene catalysts that can prepare α-olefin/DVB copolymers with a linear copolymer structure, as illustrated in Eq. (4).

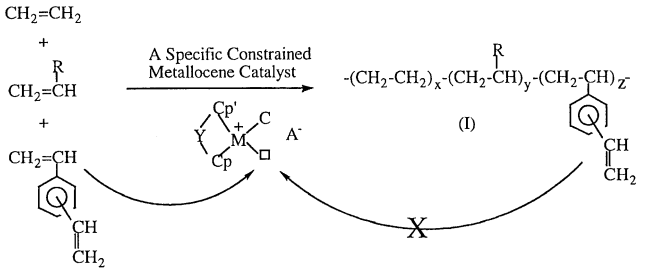

(4)

In general, the metallocene catalysts that have non-bridgeted ligand geometry, such as Cp_2ZrCl_2 with a small open active site, incorporate a very low concentration of DVB units. On the other hand, the metallocene catalysts with constrained ligand geometry, such as $[C_5Me_4(SiMe_2N^tBu)]TiCl_2$) with a large open active site, engage in serious double enchainment with both vinyl groups in the DVB monomer, which results in copolymers with branching or/and crosslinking structures. However, there is a small group of metallocene catalysts with narrowly defined openings at active sites, which can effectively incorporate DVB comonomers and produce an α-olefin/DVB copolymer with a linear copolymer structure. In other words, the catalyst can effectively incorporate DVB into the polymer through single enchainment, and no reactivity to the styrenic units already existed in the polymer.

The ideal α-olefin/DVB copolymer would have a linear polymer structure with narrow molecular weight and composition distributions, and the vinyl/phenyl (VN/PH) mole ratio in the copolymer would be nearly unity. Fig. 3 shows a ^{1}H NMR spectrum of two PE copolymers (PE-DVB) containing 1.5 and 7.2 mol% of DVB units. Four chemical shifts were observed at near 5.3, 5.8, 6.8, and 7.0–7.4 ppm (with the integrated peak intensity ratio near 1:1:1:4), corresponding to three individual vinyl protons and four aromatic protons in the pending styrene unit.

Table 5 summarizes the experimental results of terpolymerization reactions of ethylene, propylene, and DVB by using $Et(Ind)_2ZrCl_2$/MAO catalyst. High DVB incorporation was observed in all reactions — up to 20 mol% of DVB units in the EP-DVB terpolymer has been prepared. In addition, all of the terpolymers were completely soluble in common organic solvents, such as hexane, toluene, and tetrahydrofuran (THF). In general, the prepared EP-DVB terpolymers have a relatively well-defined molecular structure with narrow molecular weight and composition distributionsThe intergrated peak intensity ratio indicates that the mole ratio of vinyl/phenyl moieties (UN/PH) is nearly equal.

Fig. 4 compares the GPC curves of the EP copolymer (E: 64.8 mol%, P: 35.2 mol%) and the EP-DVB terpolymer (E: 63.7 mol%, P: 33.4 mol%, DVB: 2.9 mol%) prepared under identical reaction conditions, except for the addition of the DVB monomer. Both polymers have similar molecular weight distributions ($M_w/M_n \sim 2$), indicating nearly ideal reaction conditions. The DSC results also showed a homogeneous terpolymer microstructure with no detectable melting point (T_m) and a sharp glass transition temperature (T_g) with a flat baseline in each terpolymer.

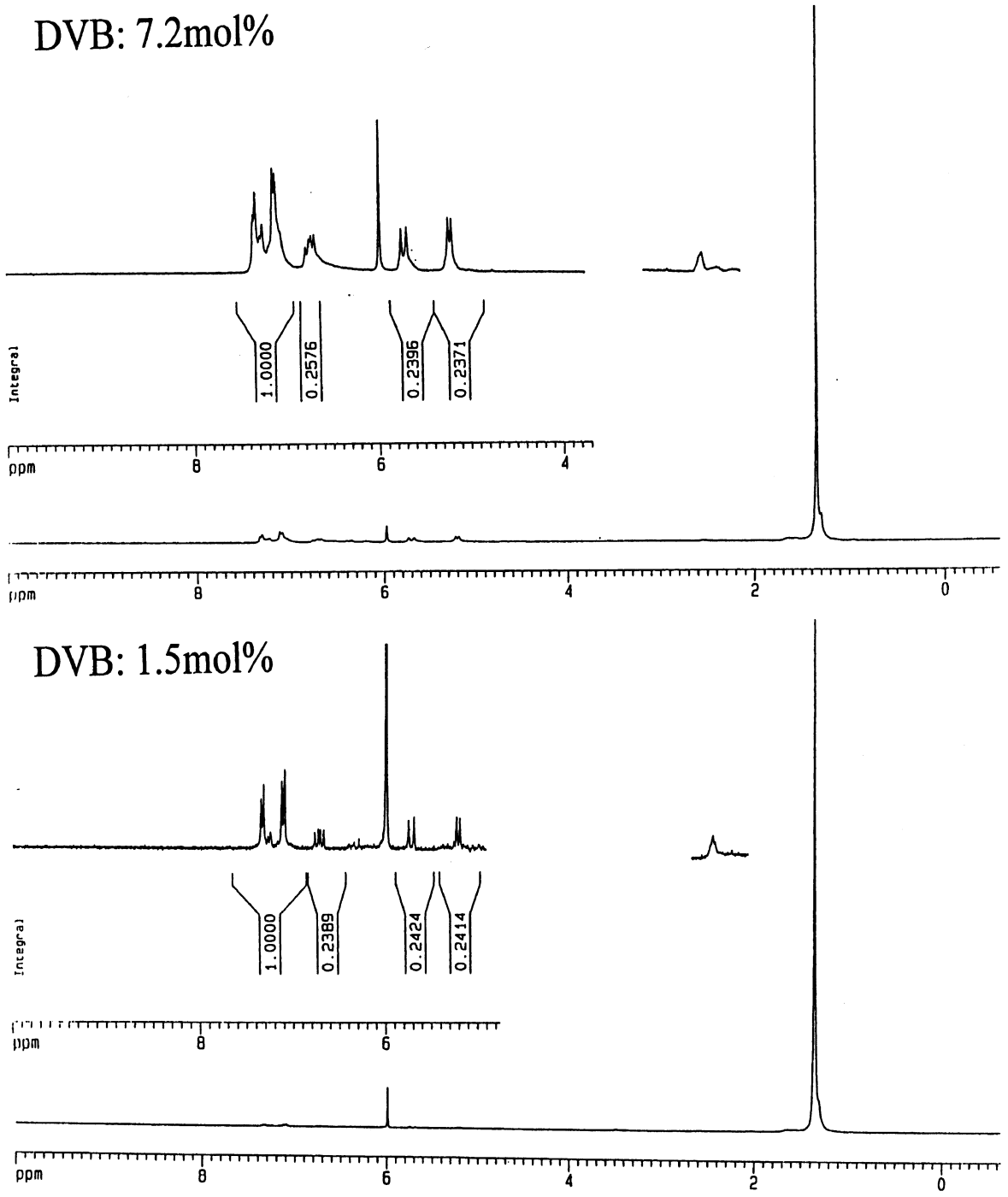

Fig. 3. ^{1}H NMR spectra of PE-DVB copolymers containing 1.5 and 7.2 mol% of DVB units.

Table 5
A Summary of terpolymerization (polymerization condition: [cat] = 2.5×10^{-6} mol; [MAO]/[Zr] = 3000; solvent: 100 ml hexane; temperature: 50°C; pressure: 30 psi; time: 15 min) of ethylene, propylene, and divinylbenzene using an $Et(Ind)_2ZrCl_2$/MAO catalyst

Monomer feed		Catalyst[a] activity	Terpolymer composition (mol%)				T_g (°C)
Mixed C_2/C_3 (psi)	DVB (mol/l)		C_2	C_3	DVB	VN/PH	
40/60	0.1	2780	56.4	42.5	1.1	95.0	−50.6
40/60	0.3	2000	59.3	39.0	1.7	93.2	−47.3
40/60	0.6	1650	62.4	32.9	4.7	97.0	−31.3
40/60	1.2	1230	56.0	22.9	21.1	98.0	−21.6
60/40	0.3	1810	67.8	30.6	1.6	97.0	−36.4
60/40	0.6	1710	65.3	30.3	4.4	95.2	−29.0

[a] Catalyst activity: Kg/mol Zr.h.

6. Synthesis of polyolefin containing a reactive end group

It is always a scientific challenge to prepare polymer having a terminal functional group, which offers an opportunity to serve as a building block for constructing multi-segmented polymers. In chemistry, the general method of preparing this class of polymers has been based on living polymerization [56–60] with a chemical reaction to convert living chain end to a functional group. In our laboratory, we have developed a very convenient and effective route to prepare polyolefin containing a borane or *p*-MS terminal group by in situ chain transfer reaction during the metallocene polymerization process. With the

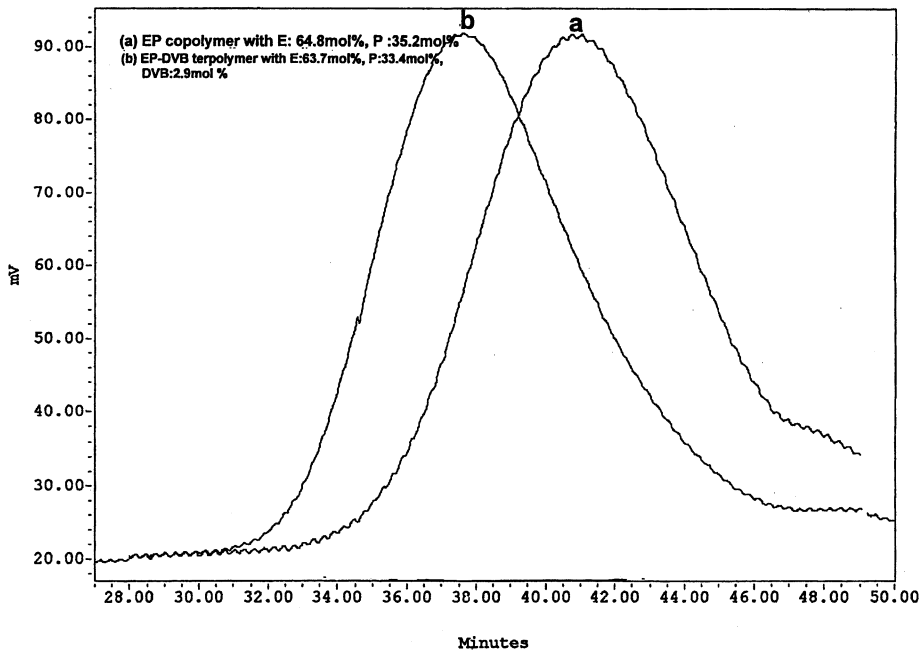

Fig. 4. GPC Curves of (a) EP copolymer and (b) EP-DVB terpolymer.

appropriate chain transfer agent (CT), it's possible to have a chain transfer reaction that in situ takes place without changing the rate of polymerization. Each catalyst can produce multiple polymer chains as usual, and the polymer chain produced has a terminal group (the residue of the chain transfer agent). Usually, the polymer's molecular weight is reversibly proportional to the [CT]/[monomer] ratio. This chemistry is a potential drop-in technology with only a small modification to current processes, and might also be applicable to all polyolefin (PE, PP, *s*-PS, etc.) cases.

6.1. Polyolefins containing a borane end group [50,51]

The application of organoboranes (containing B–H moiety) as the chain transfer agents was formulated with several intriguing questions and objectives in mind. With the knowledge of facile ligand exchange of B–H with many metal-alkyl groups, it is very possible that the B–H group has a high reactivity with M–C active sites, as illustrated in Eq. (5).

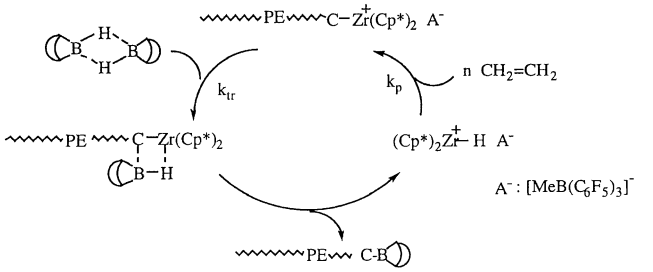

(5)

There are two concerns in the B–H chain transfer reaction, namely, hydroboration reaction of the B–H group to α-olefin monomers and ligand exchange reaction between borane and the aluminium-alkyl co-initiator. It is known that the borane compounds containing B–H groups usually form a stable dimer (unreactive to olefins) in hexane and toluene solvents that are used in metallocene polymerizations. No reaction between borane and α-olefin is expected during the polymerization. On the other hand, we can use a perfluoroborate co-initiator instead of MAO or alumium-alkyl compounds, which are stable with most alkylborane compounds. Therefore, the B–H moiety in dialkylborane can engage a chain transfer reaction by ligand exchange between B–H and M–C (M: transition metal), as illustrated in Eq. (5). Each PE chain (PE-*t*-B) will have a terminal borane group [50] if the chain transfer reaction is the dominant termination reaction, and the molecular weight of the borane-terminated polymer will be reversally proportional to the concentration of borane chain transfer agent.

Table 6 summarizes the experimental results of ethylene polymerization in the presence of 9-BBN using two metallocene catalysts, $[Cp^*_2ZrMe]^+[MeB(C_6F_5)_3]^-$ and $[Cp^*_2ZrMe]^+[B(C_6F_5)_4]^-$ ($Cp^* = \eta^5$-C_5H_5, ηs^5-Me_5C_5). To maintain the constant [borane]/[ethylene] feed ratio, the reactions were carried out with rapid mixing and a short reaction time, about a three to five minutes reaction time. Basically, higher concentrations of a 9-BBN chain transfer agent resulted in lower molecular weights of the resulting PE. The polymer molecular weight distribution is generally narrow, which is consistent with single site polymerization process. The catalyst activity was also depressed in the presence of 9-BBN, which may reflect the competitive coordination at metallocene active sites between monomer and chain transfer agents. For analytical studies, a PE-*t*-B polymer was usually oxidized by $NaOH/H_2O_2$ to form a hydroxy-terminated polymer (PE-*t*-OH).

Fig. 5 shows the plot of polymer molecular weight (M_n) vs. the mole ratio of ethylene/9-BBN for the

Table 6
Metallocene-activated ethylene polymerization (pressure = 1 atm; [ethylene] = 0.11 M) in the presence of 9-BBN as the chain transfer agent (Reproduced with permission from J. Am. Chem. Soc. 1999;121:6763. Copyright 1999 Am. Chem. Soc.)

Run	Catalyst	9-BBN (mM)	Time (min)	Yield (g)	Catalyst[a] activity	M_n[b] ($\times 10^{-3}$)	M_w/M_n
1	$[Cp^*_2ZrMe]^+[MeB(C_6F_5)_3]^-$	0	3	3.50	2333	85.2	2.0
2	$[Cp^*_2ZrMe]^+[MeB(C_6F_5)_3]^-$	3.0	3	2.01	1333	76.0	2.4
3	$[Cp^*_2ZrMe]^+[MeB(C_6F_5)_3]^-$	4.5	3	2.05	1366	55.5	2.9
4	$[Cp^*_2ZrMe]^+[MeB(C_6F_5)_3]^-$	7.5	3	1.45	1033	42.2	2.6
5	$[Cp^*_2ZrMe]^+[MeB(C_6F_5)_3]^-$	7.5	5	2.02	1333	45.8	2.6
6	$[Cp^*_2ZrMe]^+[MeB(C_6F_5)_3]^-$	12.0	3	1.20	800	19.4	2.7
7	$[Cp^*_2ZrMe]^+[MeB(C_6F_5)_3]^-$	18.0	3	0.75	500	8.9	3.2
8	$[Cp^*_2ZrMe]^+[MeB(C_6F_5)_3]^-$	23.4	3	0.25	167	3.7	4.0
9	$[Cp^*_2ZrMe]^+[B(C_6F_5)_4]^-$	4.5	3	2.00	1333	59.4	2.6
10	$[Cp^*_2ZrMe]^+[B(C_6F_5)_4]^-$	7.5	3	1.51	1000	46.2	2.5
11	$[(Ind)_2ZrMe]^+[MeB(C_6F_5)_3]^-$	7.5	3	1.90	1267	43.9	2.3
12	$[Cp_2ZrMe]^+[MeB(C_6F_5)_3]^-$	7.5	3	2.50	1667	46.9	2.1

[a] Catalyst activity = kg of PE/mol of catalyst.atm.h.
[b] By GPC in 1,2, 4-trichlorobenzene vs. polystyrene standards.

comparative runs 2–8 in Table 6. The polymer's molecular weight is almost linearly proportional to the molar ratio of [ethylene]/[9-BBN]. It is clear that the chain transfer reaction with 9-BBN (with rate constant k_{tr}) is the dominant termination process, and competes with the propagating reaction (with rate constant k_p). The degree of polymerization (X_n) follows a simple comparative equation $X_n = k_p[\text{olefin}]/k_{tr}[\text{9-BBN}]$ with a chain transfer constant $k_{tr}/k_p \sim 1/75$. The existence of a borane terminal group in PE was also evidenced by the NMR spectrum of a low molecular weigth PE-*t*-OH.

Similar B–H chain transfer reactions can be applied to other metallocene-mediated olefin polymerizations. One example is the synthesis of borane-terminated syndiotactic polystyrene (s-PS-*t*-B) [51]. Table 7 shows several $[Cp^*TiMe_2]^+[MeB(C_6F_5)_3]^-$ mediated polymerizations of styrene with the presence of 9-BBN. The effects of the chain transfer reaction are clearly revealed by the reduction of the polymer's molecular weight in the presence of 9-BBN. Basically, the higher the concentration of 9-BBN chain transfer agent used, the lower the molecular weight of the resulting PE. The catalyst activity was somewhat depressed if a high concentration of 9-BBN was presented in the system, which may reflect the competitive coordination at the titanocene active sites between monomers and chain transfer agents. It is very interesting to note that the syndiotacticity and melting temperatures of all *s*-PS-*t*-B polymers are similar to those of the *s*-PS polymer. The 9-BBN chain transfer agent did not interfere with the regio- and stereo-selective insertion process.

6.2. Polyolefins containing a p-methylstyrene end group [52]

Recently, we have also discovered a new polymerization process to prepare *p*-methylstyrene (*p*-MS) terminated polyolefins. The process involves contacting α-olefin ($>C_3$) with *p*-MS and hydrogen simultaneously in the presence of some metallocene catalysts containing a specific bridged Cp^* ligand. Ironically, the desirable metallocene catalysts usually show very poor styrene incorporation in the copolymerization reaction between propylene and styrene. The reaction mechanism involved in forming

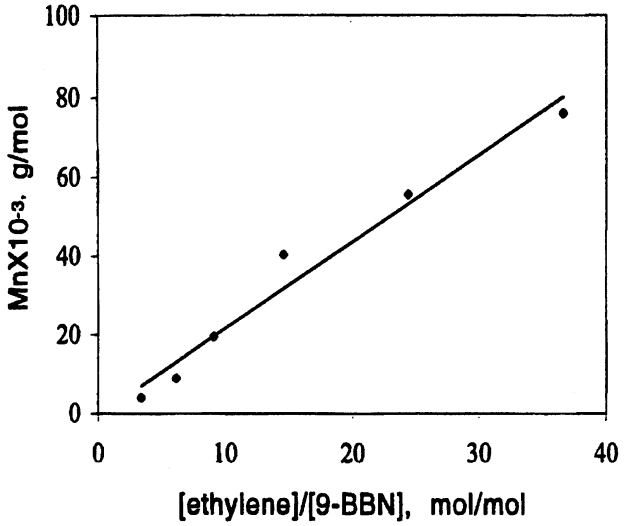

Fig. 5. A plot of the average molecular weights (Mn) of PE-*t*-B polymers vs. the mole ratio of [ethylene]/[9-BBN] in the feed (runs 2–8 in Table 6). (Reproduced with permission from J. Am. Chem. Soc. 1999;121:6763. Copyright 1999 Am. Chem. Soc.)

the *p*-MS terminated polyolefin may be exemplified by the polymerization of propylene in the presence of *p*-MS and H_2 chain transfer agents using a rac-Me_2Si[2-Me-4-Ph(Ind)]$_2ZrCl_2$/MAO catalyst, as illustrated in Eq. (6).

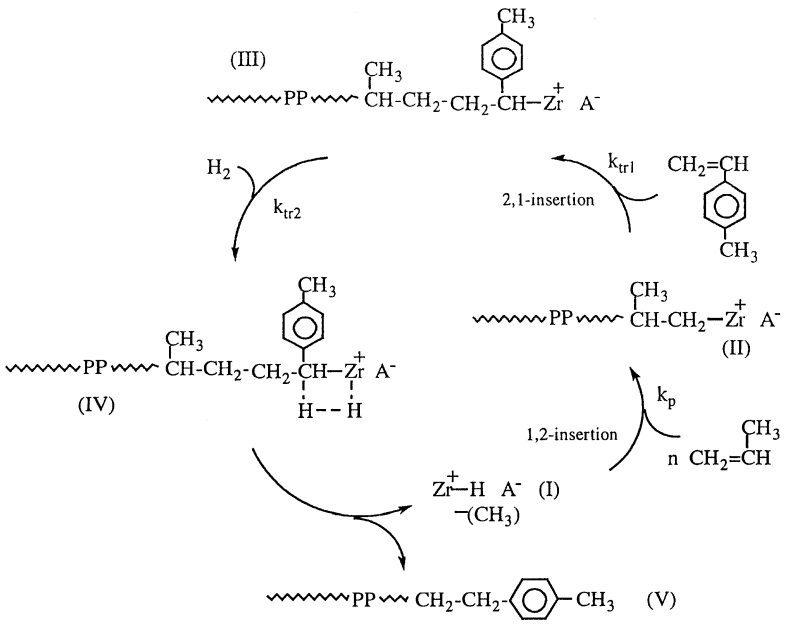

(6)

During the polymerization of propylene (with 1,2-insertion manner) the propagation Zr–C site (II) can also react with *p*-methylstyrene (with 2,1-insertion manner) to form *p*-methylstyrene terminated PP (III). The catalytic Zr–C site in compound (III) becomes inactive to both propylene and *p*-methylstyrene

Table 7
$[Cp^*TiMe_2]^+[Me(B(C_6F_5)_3]^-$ — activated styrene syndiospecific polymerization in the presence of 9-BBN as a chain transfer agent (styrene = 10 ml, catalyst concentration = 10 μmol) (Reproduced with permission from Macromolecules 1999;32:8689. Copyright 1999 Am. Chem. Soc.)

Run	9-BBN (μmol)	Reaction time (min)	Yield (g)	Catalyst activity[a]	Syn.[b] (%)	T_m (°C)	$[\eta]$	M_w (g/mol)
1	25	3	1.3	2600	97.0	270	1.270	460,000
2	50	3	1.4	2800	96.2	271	0.806	240,000
3	100	3	1.3	2600	95.8	270	0.580	150,000
4	150	3	1.1	2200	95.2	271	0.373	80,000
5	200	3	0.8	1600	93.4	270	0.340	70,000
6	300	3	0.5	1000	94.7	272	0.188	30,000
7	400	3	0.3	600	95.0	270	0.116	15,000
8	500	3	0.1	200	93.2	270	0.087	10,000

[a] Catalyst activity = kg of *s*-PS/mol of Ti·h.
[b] Syndiotactic index was determined by ^{13}C NMR.

[302] due to the combination of steric hindrance between the active site (Zr–C) and the incoming monomer (propylene with 1,2-insertion), and the formation of complex between the adjacent phenyl group and the Zr^+ ion. On the other hand, with the presence of hydrogen the dormant Zr–C site (III) can react with hydrogen to form PP-*t*-*p*-MS (V) and regenerate a Zr–H species (I) that is capable of reinitiating the polymerization of propylene and continuing the polymerization cycle. Overall, the polymerization process resembles a sequential chain transfer reaction — first to styrene (or styrene derivative) and then hydrogen — during the metallocene mediated propylene polymerization. This process not only produces PP with a terminal *p*-MS unit, but also maintains high catalyst activity. The molecular weight of the resulting polymer is proportional to the [propylene]/[*p*-MS] ratio.

Table 8 summarizes the results of *p*-methylstyrene terminated polypropylene (PP-*t*-*p*-MS) using a rac-$Me_2Si[2\text{-Me-4-Ph(Ind)}]_2ZrCl_2$/MAO catalyst in the presence of *p*-MS and hydrogen chain transfer agents. The systematic study was conducted to evaluate the effect of hydrogen and *p*-MS concentrations on the catalyst activity and polymer molecular weight. All comparative reaction sets show that hydrogen is necessary to complete the chain transfer reaction to *p*-MS during the metallocene-mediated polymerization of propylene. In general, the change of hydrogen concentration does not affect the molecular weight and molecular weight distribution of the resulting *p*-MS terminated PP polymers. However, a sufficient quantity of hydrogen, which increases with the increasing of [*p*-MS], is needed to maintain high catalyst activity and *p*-MS conversion.

Fig. 6 (left) compares the GPC curves of PP-*t*-*p*-MS polymers with a PP homopolymer. All polymers were prepared under the same reaction conditions, except for varying the quantity of the *p*-MS chain transfer agent. An appropriate concentration of hydrogen was also introduced in each chain transfer reaction to assure the completion of the polymerization cycles. The GPC curves show the systematic reduction of the polymer molecular weight, along with the increase of the *p*-MS concentration. The low molecular weight PP-*t*-*p*-MS (M_n as low as a few thousandths) that has been prepared is a well-defined polymer with narrow molecular weight distribution ($M_w/M_n \sim 1.7$). In fact, the molecular weight distribution of PP-*t*-*p*-MS gradually reduced along with the reduction in the polymer molecular weight. All experimental results clearly indicate effective chain transfer reactions.

The kinetic constants during the polymerization can be obtained from Fig. 6 (right), which shows the

Table 8
A summary of PP-*t*-*p*-MS polymers prepared (reaction conditions: 50 ml toluene, propylene (100 psi), [Zr] = 1.25×10^{-6} mol/l, [MAO]/[Zr] = 3000, temperature = 30°C, time = 15 min) by the combination of a rac-Me_2Si[2-Me-4-Ph(Ind)]$_2ZrCl_2$/MAO catalyst and *p*-MS/hydrogen chain transfer agents

Run	*p*-MS (M)	H_2 (psi)	Yield (g)	Catalyst activity[a]	*p*-MS in PP (mole%)	*p*-MS Conversion (%)	Mn ($\times 10^{-3}$)	PDI (Mw/Mn)
Control 1	0	0	26.94	86,208	0	–	77,600	2.9
Control 2	0.0305	0	0.051	163	0.16	0.05	59,700	3.4
1	0.0305	2	3.80	12,160	0.14	8.30	55,500	2.4
2	0.0305	6	8.04	25,728	0.15	18.83	54,800	2.5
3	0.0305	12	12.04	38,528	0.15	28.19	55,400	2.3
4	0.0305	35	24.67	78,944	0.13	50.05	34,600	2.8
Control 3	0.076	0	~ 0	–	–	–	–	–
5	0.076	6	0.91	2912	0.40	2.33	27,600	2.1
6	0.076	12	1.69	5408	0.41	4.33	25,900	2.3
7	0.076	20	8.81	28,192	0.43	23.65	20,500	2.3
8	0.076	35	10.52	33,664	0.41	26.86	25,800	2.3
Control 4	0.153	0	~ 0	–	–	–	–	–
9	0.153	12	0.35	1120	0.66	0.72	10,000	2.0
10	0.153	20	3.81	12,192	0.61	7.26	11,700	2.0
11	0.153	35	4.41	14,112	0.63	8.67	9700	1.9

[a] Catalyst activity = kg of PP/mol of catalyst.h.

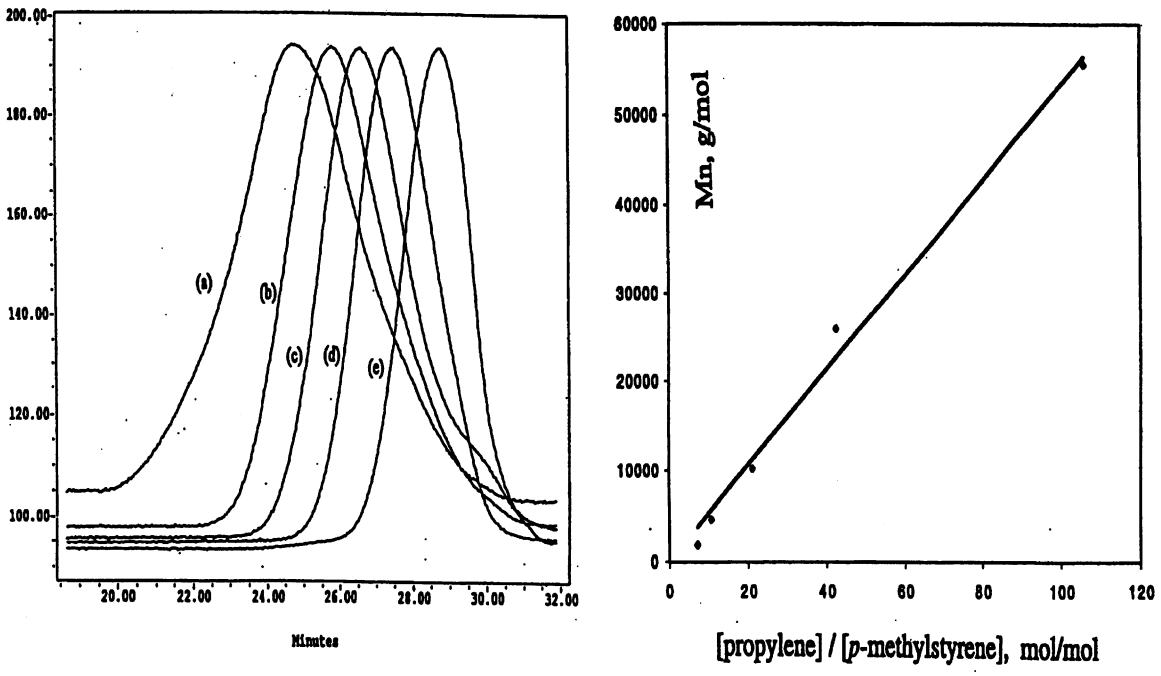

Fig. 6. Left: GPC curves of (a) PP ($M_n = 77.6 \times 10^3$) and several PP-*t*-*p*-MS polymers with M_n of (b) 54.8×10^3, (c) 25.9×10^3, (d) 10×10^3, and (e) 4.6×10^3 g/mol. Right: the plot of PP-*t*-*p*-MS molecular weight to mole ratio of [propylene]/[*p*-MS]. (Reproduced with permission from J. Am. Chem. Soc. 2001;123:4871. Copyright 2001 Am. Chem. Soc.)

plot of the PP-*t*-*p*-MS molecular weight to the mole ratio of [propylene]/[*p*-MS]. The linear relationship between M_n and [propylene]/[*p*-MS] clearly indicates that the chain transfer reaction to *p*-MS (with rate constant k_{tr}) is the dominant termination process, and competes with the propagating reaction (with rate constant k_p). The degree of polymerization (X_n) follows the equation $X_n = k_p[\text{propylene}]/k_{tr}[p\text{-MS}]$ with a chain transfer constant $k_{tr}/k_p \sim 1/6.36$. It is very interesting to note that the same chain transfer reaction scheme can be applied to many styrenic derivatives, including the ones containing masked functional group, which are very desirable in some polymer modification reactions.

7. Synthesis of polyolefin graft copolymers

As discussed, the major objective of developing reactive polyolefins is to prepare functional polyolefins with graft and block structures. These polymers, containing high concentration of functional (polar) groups and persisting the desirable polyolefin properties, are very effective interfacial agents to improve the compatibility of polyolefin with other materials.

In the graft copolymer structure, the polymer contains a polyolefin backbone and several functional polymer side chains, such as PMMA, PVA, and PCL. In general, the chemistry to prepare polyolefin graft copolymers is very limited. Numerous approaches, based on post polymerization process, have been employed in forming polyolefin graft copolymers. Ionizing radiation (X-ray, γ-rays, and e-beams) in the presence of air, ozone, UV with accelerators, and free radical initiators [61,62] have all been used

to form polymeric peroxides. When heated in the presence of monomers, some polymeric peroxides initiate graft polymerization. However, these high-energy reactions lead to many side reactions, such as crosslinking and chain cleavage. In most cases, the structure and composition of copolymers are difficult to control given the considerable amounts of ungrafted homopolymers.

By far, the most effective route for preparing functional polyolefin graft copolymers is by employing reactive polyolefin intermediates, containing borane [63–67], *p*-methylstyrene [42–44], and divinylbenzene [52] reactive side groups. The reactive groups provide the selective sites (serving as initiators, monomers, or termination agents) in the graft reaction of functional monomers. The combination of these three reactive polyolefin approaches (discussed in this section) offers a comprehensive coverage of polyolefin graft copolymers with well-defined molecular structure, i.e. controlled graft density and graft length.

7.1. Living radical graft-from polymerization via borane side groups

As illustrated in Eq. (7), the alkyl-9-BBN side groups in polyolefin (see Section 5.1) can then be spontaneously oxidized to a peroxide (B–O–O–C) moiety (I) even at very low temperature (−65°C). Due to the unfavorable ring strain increase by inserting oxygen into the C–B bonds in the bicyclic ring of 9-BBN, which destroys the stable double chair-form structure, the oxidation reaction selectively takes place at the C–B bond [68,69] in the linear alkyl group to produce peroxyborane (C–O–O–B) (I).

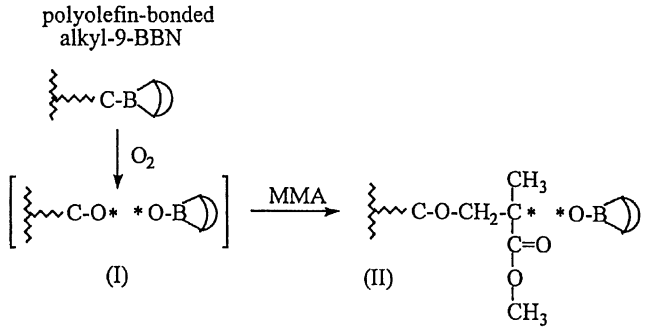

(7)

The peroxyborane (I) behaves very differently from regular benzoyl peroxides, and consequently decomposes by itself even at ambient temperature. The decomposition reaction follows the homolytical cleavage of peroxide to generate an alkoxy radical (C–O ∗) and a borinate radical (B–O ∗). The alkoxyl radical (C–O ∗) is very reactive and can then be used for the initiation of radical polymerization with the presence of free radical polymerizable monomers, such as methacrylates, vinyl acetate, acrylonitrile, etc., at ambient temperature. On the other hand, the borinate radical (B–O ∗), stabilized by the empty p-orbital of boron through back-donating electron density, is too stable to initiate polymerization. However, the borinate radical may form a weak and reversible bond with the growing chain end during the polymerization reaction. Upon the dissociation of the electron pairs in the resting state, the growing chain (II) can then react with monomers to extend the polymer chain to form graft copolymer. This living polymerization process minimizes the undesirable chain transfer reaction and termination (coupling and disproportional) reaction between the two growing chain ends, which result in the formation of homopolymers and crosslinked material. In most cases, the resulting graft copolymers are completely soluble and processible. The graft length (PMMA side chain) is basically controlled by the MMA concentration and reaction time. Some interesting graft polymers - including PE-*g*-PVA, PE-*g*-PMMA, PP-*g*-PMMA,

Table 9
A summary of PP-*g*-PMMA graft copolymers [66]

Run number	9-BBN in PP (mol%)	O_2 (ml/h)	Monomer/solvent	Reaction time (h)	MMA in PP (mol%)
1	0.5	1.5/12	MMA (neat)	48	66
2	0.5	3.0/1	MMA (neat)	2	6
3	0.5	1.4/3	MMA/THF	12	52
4	0.5	6 (at once)	MMA (neat)	48	1.5
5	0.5	Diffusion	MMA/THF	48	12

PP-*g*-PMA, PP-*g*-PVA, PP-*g*-SMA (SMA: styrene/maleic anhydride alternating copolymer), EP-*g*-PMMA, EP-*g*-SMA and Butyl-*g*-PMMA — have been synthesized with controllable compositions and molecular microstructures [63–67].

Table 9 summarizes the experimental results of PP-*g*-PMMA copolymers. The comparison among runs (A-1–A-4) shows the relationship of the addition of oxygen to the graft efficiency. Even though the final stoichiometry of oxygen to boron should be 1:1, the best results in this heterogeneous reaction system are realized when the O_2 is introduced slowly so that $O \ll B$ at any time. Excess O_2 is not only a poison for free radical polymerizations, but also leads to over-oxidation to boronates and borates which are poor free radical initiators at room temperature. The polarity of the solution also effects the graft reaction. THF is a very good solvent in this reaction. Non-polar solvents, such as benzene, slow down the graft-from reaction, which may be due to the solubility of O_2 in the solvent. In the run A-5, the oxygen was introduced by diffusion of air through the rubber septum that was tightly installed on the top of the reactor. The insufficient O_2 in this process leads to low percentage of PMMA formation.

Fig. 7 compares the IR spectra of three PP-*g*-PMMA graft copolymers and a corresponding PP-OH. All of them were derived from the same copolymer contained 0.5 mol% borane monomers. PP-OH polymer was obtained by converting borane groups to hydroxy groups, and all graft copolymers were prepared under the same reaction conditions expect for reaction time. The IR spectrum of PP-OH is basically indistinguishable from that of *i*-PP because of the extremely low concentration of hydroxy groups. On the other hand, the strong absorption band at 1730 cm^{-1}, corresponding to ester groups, clearly shows the existence of PMMA in the graft copolymers. A high concentration (>65 mol%) of PMMA can be incorporated into PP by a small quantity (0.5 mol%) of borane groups. The PMMA content increases with the reaction time, which indicates the living free radical polymerization process, and the graft length is basically controlled by the reaction time and monomer concentration.

Similar graft-from reactions have been extended to other polyolefins. Satisfactory results were obtained in both homogeneous (PE, PP, and PB cases) and heterogeneous (PO, EP, and Butyl rubber cases) reaction conditions [70,71]. In one homogeneous case, a commercial EPDM rubber was used to prepare EP-*g*-PMMA graft copolymers. Fig. 8 compares the ^1H NMR spectra of the resulting EP-*g*-PMMA copolymers and the starting EPDM rubber, poly(ethylene-*co*-propylene-*co*-1,4-hexadiene). The chemical shift at 3.6 ppm in Fig. 11(b) and (c) corresponds to the methyl groups (CH_3O) in PMMA. The chemical shifts between 2.1 and 0.7 ppm include all of the protons in EP and five of the protons in the methyl group located on the PMMA backbone. The copolymer composition was calculated by the ratio of the two integrated intensities at 3.6 and 0.7–2.1 ppm and the number of protons both chemical shifts represent. Fig. 11(b) and (c) indicate 28 and 52 mol % PMMA in EP-*g*-PMMA copolymers, respectively.

The DSC curve of the EP-*g*-PMMA copolymer (with a 50/50 composition) shows two glass transition

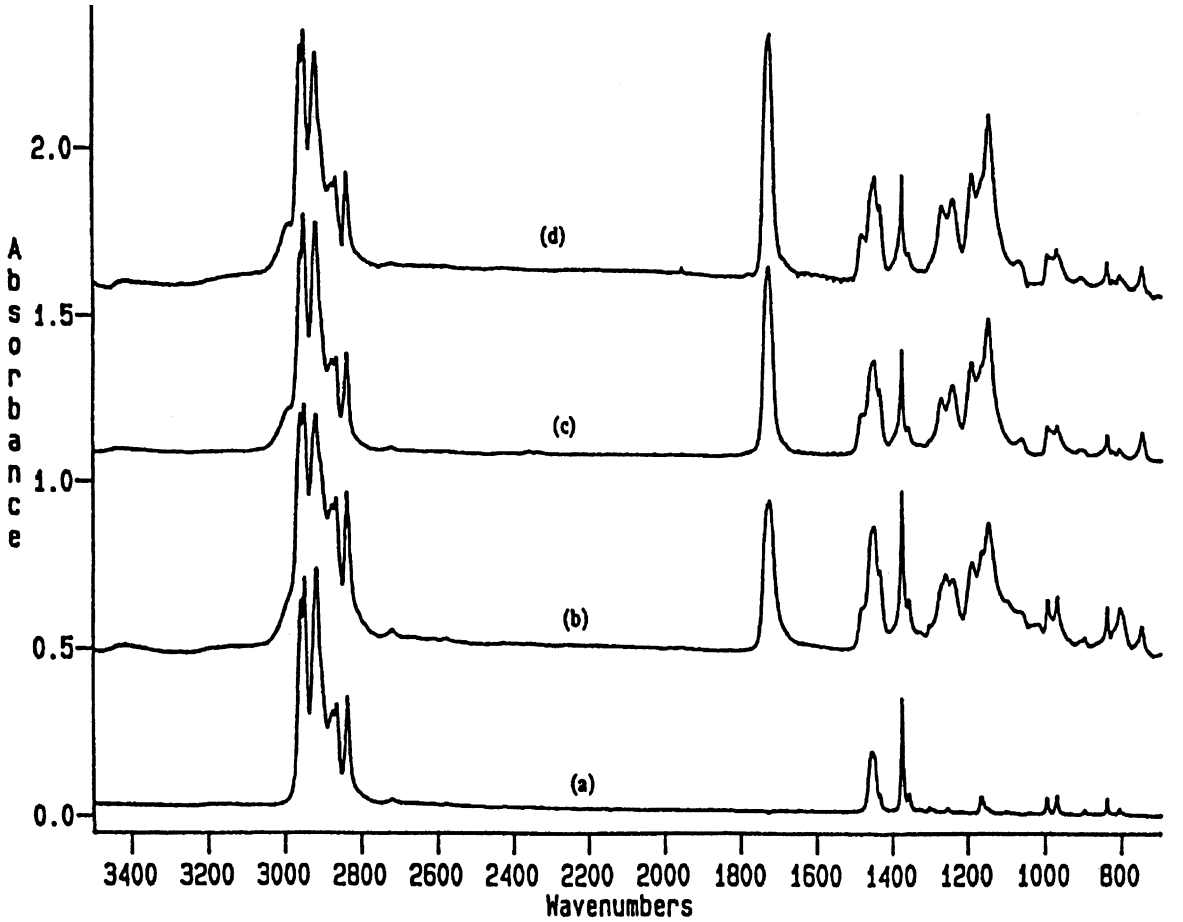

Fig. 7. IR spectra of (a) PP-OH with 0.5 mol% OH groups and three PP-*g*-PMMA graft copolymers containing (b) 20, (c) 52, and (c) 66 mol% MMA. (Reproduced with permission from Macromolecules 1993;26:3467. Copyright 1993 Am. Chem. Soc.)

temperatures (T_g), −47 and +130°C, corresponding to the starting EPDM rubber and PMMA homopolymer, respectively. This result indicates a clear phase separation between the EP backbone and the PMMA side chains. The copolymer backbone must have enough consecutive sequences of EP backbone units to form separate domains. The side chain must be a high molecular weight polymer with a microstructure similar to that of PMMA homopolymer. The clear phase separation with hard (polar) and soft (non-polar) domains is a very interesting molecular structure. In fact, most of the graft copolymers behave like thermoplastic elastomers.

7.2. Living anionic graft-from polymerization via p-methylstyrene side groups [72]

As discussed in Section 5.2, polyolefins containing *p*-MS groups have been prepared via metallocene copolymerization reactions, the copolymers cover a wide range of compositions and narrow molecular weight and composition distributions. Usually, a low concentration (<1 mol%) *p*-MS in the copolymer

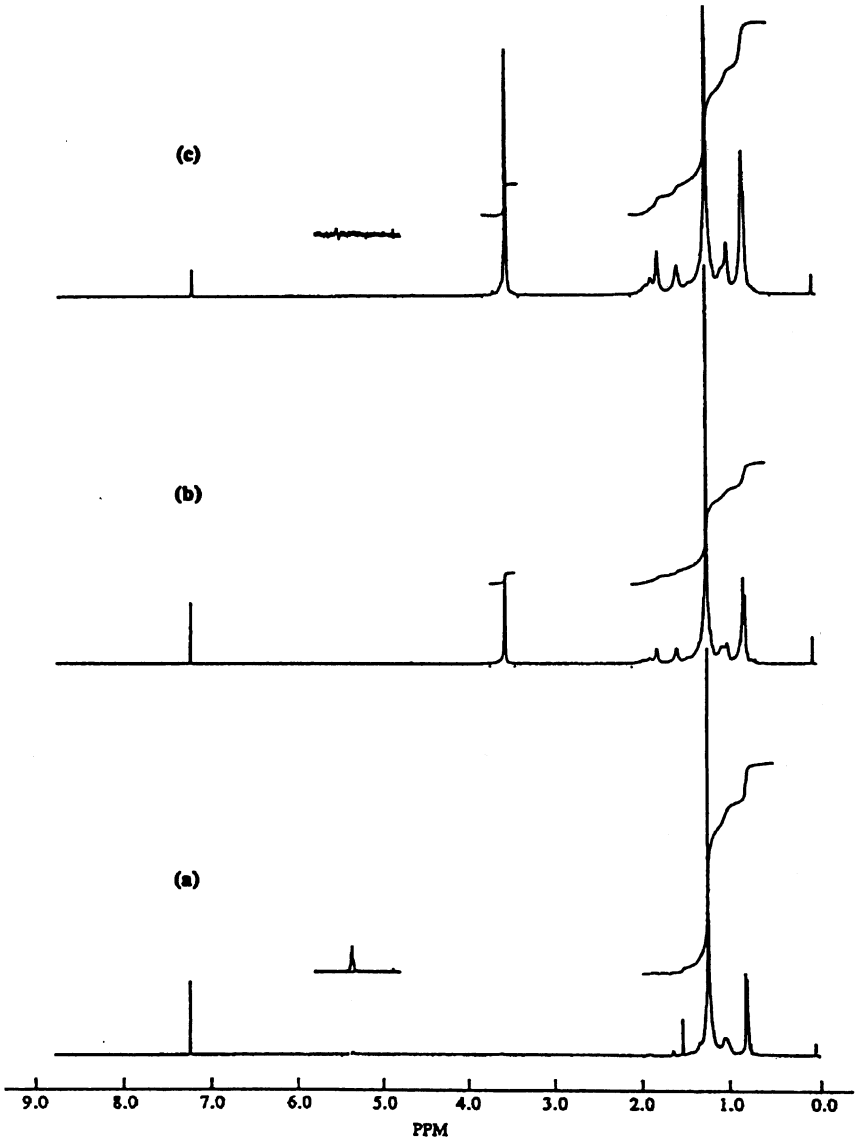

Fig. 8. Comparison of the ^{1}H NMR spectra of (a) EPDM and two resulting EP-*g*-PMMA copolymers containing (b) 28 and (c) 52 mol% PMMA. (Reproduced with permission from Macromolecules 1994;27:26. Copyright 1994 Am. Chem. Soc.)

is preferred for the preparation of graft copolymer because the resulting graft copolymer will have low graft density and long graft length. As illustrated in Eq. 8, the *p*-MS groups in PE can be effectively metallated at ambient temperature. The lithiated PE-*p*-MS copolymer contain several polymeric anions that are homogeneously distributed in the polymer chain. The living anionic graft-from reactions were generally carried out at ambient temperature by suspending the lithiated PE-*p*-MS copolymer in cyclohexane in the presence of the monomers. After the polymerization reaction, the crude product was vigorously extracted to remove any ungrafted homopolymer. In all cases, the homopolymer fraction

was negligible. The insolubility of the crystalline PE-*p*-MS copolymer at room temperature allows for maximum removal of the unreacted lithiation reagent after the metallation reaction. The combination of pure lithiated polymer and the living graft-from polymerization minimizes the formation of ungrafted homopolymer during the graft-from polymerization.

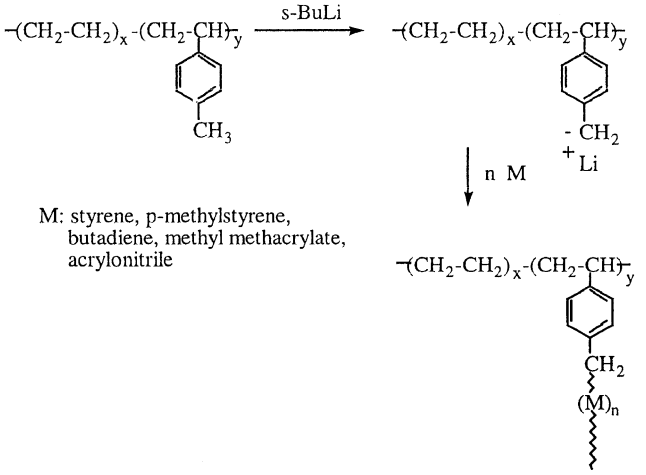

(8)

Fig. 9 shows ^{1}H NMR spectra of three resulting PE-*g*-PS graft copolymers containing 25.6, 38.1, and 43.8 mol% polystyrene, respectively. They were prepared from the same starting PE-*p*-MS polymer, containing 0.9 mol % of *p*-MS units. In contrast to the starting PE-*p*-MS, three additional chemical shifts arise in the graft copolymers at 1.55, 2.0, and 6.4–7.3 ppm corresponding to CH_2, CH, and aromatic protons in polystyrene. The quantitative analysis of the copolymer composition was calculated by the ratio of two integrated intensities between the aromatic protons ($\delta = 6.4$–7.3 ppm) in the PS side chains and the methylene protons ($\delta = 1.35$–1.55 ppm) and the number of protons both chemical shifts represent.

Table 10 summarizes the experimental conditions and results of two sets of comparative graft-from reactions, all started from the same PE-*p*-MS copolymer (containing 0.9 mol% *p*-MS) and different extend of metallation reaction. Both the yield and graft compositions (PS content) of the graft copolymer are basically proportional to the quantity of monomers used in the graft-from reaction. The good control of graft copolymer formation is obviously due to the living anionic polymerization, which effectively converts monomers to the grafted side chains. The graft density is defined as the number of grafted side chains per 1000 repeating methylene units of the PE backbone. Since this process involves living anionic polymerization and fast initiation, it is reasonable to assume that each benzylic lithium produces one PS side chain and that the side chains have a narrow molecular weight distribution. Therefore, the graft density is the same as the density of the benzylic anions. The molecular weight of the side chain is inversely proportional to the degree of metallation and proportional to the quantity of monomer used in the graft-from polymerization.

Overall, this chemistry provides a very useful route for preparing PE-*g*-PS and PE-*g*-PMS copolymers with relatively well-defined molecular structures, i.e. relatively narrow molecular weight distribution ($\bar{M}_w/\bar{M}_n = 2.5$) of the backbone and well-defined side chains. All the important factors in a graft copolymer — including graft density, graft length and copolymer composition — can be controlled during the reaction processes.

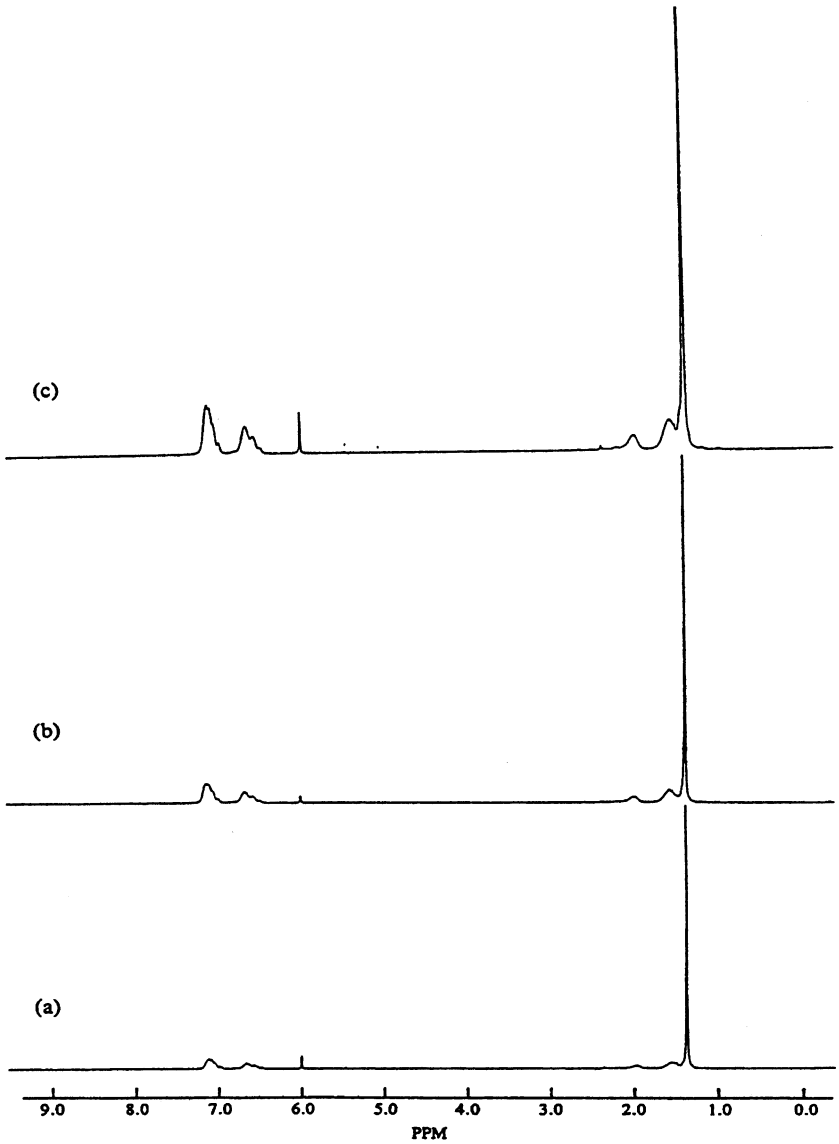

Fig. 9. ^{1}H NMR spectra of PE-*g*-PS graft copolymers with (a) 25.6, (b) 38.1, and (c) 43.8 mol% polystyrene (Reproduced with permission from Macromolecules 1997;30:1272. Copyright 1997 Am. Chem. Soc.).

It is interesting to note that as the PS graft length increases, the T_m of PE only slightly decreases. The sample B-3, containing 47.8 mol% (77.3 wt%) PS, still shows the T_m at 120.3°C. On the other hand, the heat of fusion (H_f = J/g of graft copolymer) is very dependent on the PS graft chain length. In samples B-1 and B-2, with graft chain lengths $< 12 \times 10^3$ g/mol, the heat of fusion after normalizing with the content of PE (H_f = J/g of PE) in each case is very similar to that of the pure PE sample, despite relatively high PS contents (48.9 and 58.4 wt%, respectively). The simple dilution effect seems to govern the heat of fusion in the graft copolymers. However, in samples A-1, A-2, A-3 and B-3, with the graft

Table 10
A summary of PE-*g*-PS graft copolymers (solvent: anhydrous cyclohexane (30 ml/g PE); reaction time: 1 h; temperature: 25°C)

Run number	Reaction conditions			Graft copolymers[a]					
	PE^--i^+ g	ST (g)	Yield (g)	Graft (mol%)	Graft density	Graft length	T_g (°C)	T_m (°C)	H_f J/g of graft
	Starting material[b]			0	0	0	–	127.8	199.0
A-1	1.0	1.7	2.30	25.6	0.8	23.4	103.6	121.9	60.6
A-2	1.0	2.9	3.30	38.1	0.8	41.4	103.8	120.3	41.7
A-3	1.0	4.0	3.90	43.8	0.8	52.2	103.0	120.9	31.1
B-1	1.0	1.4	2.00	20.5	2.0	6.99	84.6	126.6	99.6
B-2	1.0	2.3	2.50	27.4	2.0	10.5	91.9	123.2	80.4
B-3	1.0	4.2	4.42	47.8	2.0	23.9	103.7	120.3	25.4

[a] Graft density: # of graft/1000 carbons of backbone; graft length: 10^3 g/mol.
[b] The starting material was poly(ethylene-*co*-*p*-methylstyrene) with 0.90 mol% of *p*-MS, $\bar{M}_w = 100,000$ g/mol, $\bar{M}_w/\bar{M}_n = 2.5$.

length $>17 \times 10^3$ g/mol, the additional disorder associated with long grafted side chains becomes significant. So far, there is no theoretical explanation for the graft chain length effect on the crystallinity of the PE backbone. On the other hand, the glass transition temperature (T_g) of the PS side chains is clearly observed in DSC curves. As the molecular weight of PS increases, so does the T_g. The T_g becomes constant when the graft length exceeds 15×10^3 g/mol.

The lithiated PE-*p*-MS polymer was also used as the starting material to initiate graft-from polymerization of methyl methacrylate (MMA) and acrylonitrile (AN) in THF or cyclohexane solvents. The crude polymer products were subjected to solvent fractionation. In most cases, less than 10% of homopolymer was obtained. Table 11 summarizes the experimental results of PE-*g*-PMMA and PE-*g*-PAN. Overall, the graft-from polymerization reactions of MMA and AN are less efficient compared with those of styrene and *p*-MS. A polar solvent like THF gives poor yield at both 0 and 25°C, while a non-polar solvent such as cyclohexane gives much better results. Polar solvents may increase the nucleophilicity of the carbanion, which results in more side reactions. It is very interesting to note that the anionic polymerization of polar monomers using butyllithium as an initiator cannot achieve high

Table 11
Summary of PE-*g*-PMMA and PE-*g*-PAN Coplymers [32]

Lithiated polymer (g)	Monomer (g)	Solvent	Temperature (°C)	Time (h)	Graft copolymer (g)	PMMA or PAN content (mol%)
1.0	MMA/3.7	THF	0	1.5	1.86	20.0
1.0	MMA/3.4	THF	0	15	2.66	31.8
1.0	MMA/5.0	THF	25	5	1.90	20.1
0.8	MMA/4.0	Hexane	25	5	3.08	44.4
0.8	MMA/4.0	Hexane	0	5	2.21	33.0
1.2	AN/3.0	THF	25	1	1.60	15.0
1.2	AN/3.6	THF	25	16	2.25	32.0
1.0	AN/3.0	Hexane	25	16	2.99	51.2

polymer at ambient temperature. Usually, very low reaction temperatures ($<-20°C$) are required. In lithiated PE-*p*-MS case, the formed polymeric benzylic lithium is much more stable, and therefore minimizes the side reactions. As can be seen from Table 11, graft-from polymerization reactions of MMA and AN in the non-polar solvent cyclohexane are fairly effective and a sufficiently long graft length can be achieved even at ambient temperature. Similar graft-from polymerization of polar monomers were also observed the lithiated PP-*g*-PS polymer.

7.3. Graft-from and graft-onto polymerization involving divinylbenzene side groups

One major advantage of the α-olefin/divinylbenzene copolymers is the existence of many pending styrene groups along the backbone, which are very reactive in many chemical reactions — including free radical, cationic, anionic, and transition metal coordination processes. As illustrated in Eq. (9), the pending styrene units serve as comonomers in the graft reactions [49]. This process resembles graft-through polymerization, and the resulting graft copolymer has a polyolefin backbone and several polymer side chains that are bonded to the polyolefin at the middle of the polymer chain. The major concern of this graft reaction is the potential of crosslinking involving multiple polyolefin-bonded styrene units. Usually, the reaction has to be carried out in specific reaction conditions to obtain completely soluble graft copolymers with desirable compositions.

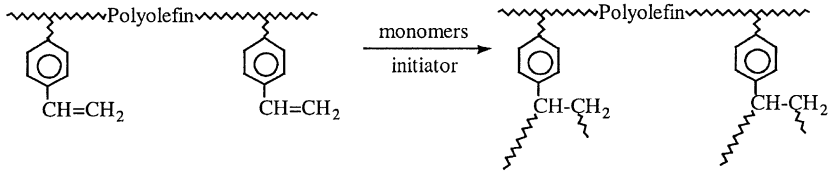

(9)

To eliminate the concerns about crosslinking reactions, it is important to design a graft reaction with the pending styrene units serving as the initiation or termination sites. In other words, the side chain polymer grafts to the backbone at its chain end, and the graft polymer basically has a similar molecular structure as those discussed in the previous sections. The following two graft reactions, involving a pending styrene unit as the anionic initiating site and metallocene terminating site, respectively, are used to illustrate the general idea.

In anionic graft-from polymerization, the process begins with a metallation reaction of DVB containing copolymer with alkyllithium (such as *n*-BuLi) to form a polyolefin containing pending benzylic anions. By limiting the alkyllithium added to the reaction to the amount required to react with all of the DVB units in the copolymer, the metallation reaction between the pending styrene unit and the alkyllithium is quantitative. In other words, no purification is needed before adding anion-polymerizable monomers to continue the living anionic graft-from polymerization process. It is very interesting to note that the anionic polymerization of various monomers, such as methyl methacrylate, can take place at room temperature without causing any detectable side reactions, which may be associated with the stable benzylic anion initiator. After achieving the desired composition of the graft copolymer, the graft reaction can be terminated by adding a proton source, such as methanol or isopropanol. Thus, by using this easily controllable living graft-from reaction technique, a variety of graft copolymer compositions with well-defined side chain segments, including random and block copolymers, have been produced that are all completely soluble in organic solvents.

Fig. 10 compares the ^{1}H NMR spectrum of a graft copolymer, having an ethylene/1-octene/DVB

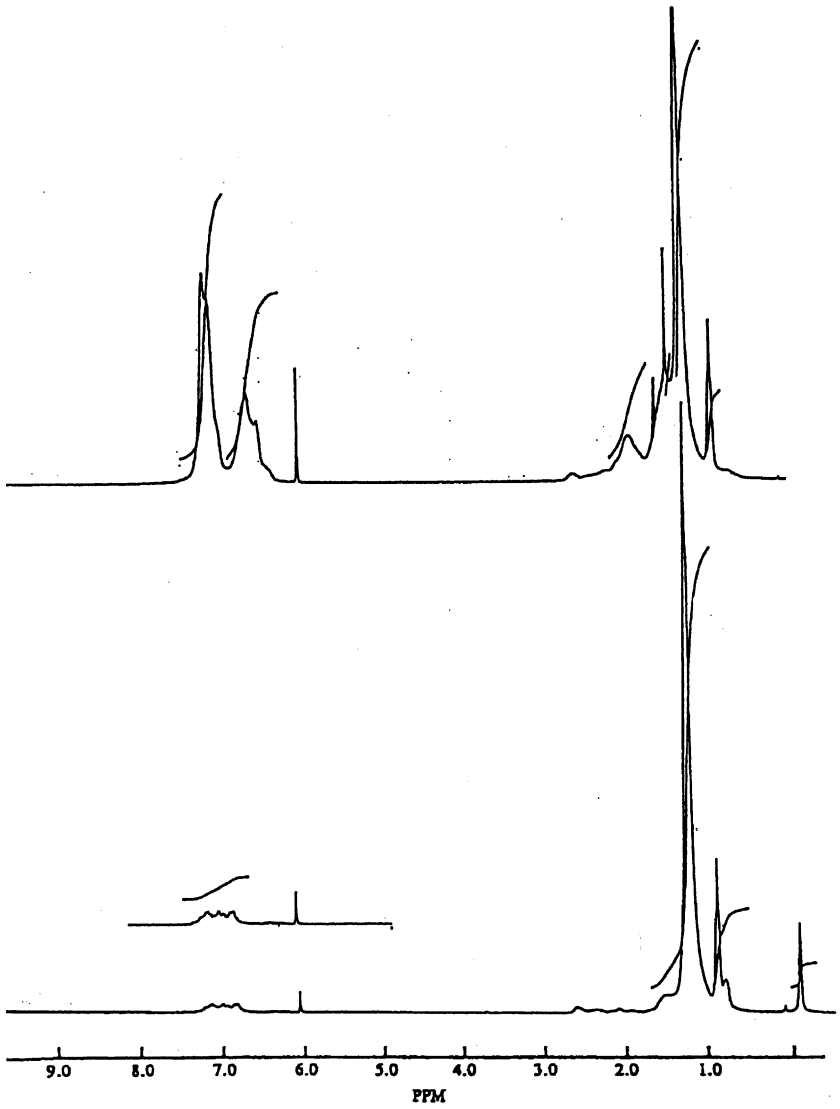

Fig. 10. ^{1}H NMR spectrum of a silylated ethylene/1-octene/DVB terpolymer (bottom) and a graft copolymer with ethylene/1-octene/DVB backbond and polystyrene side chains (top). Both polymers were derived from the same starting ethylene/1-octene/DVB terpolymer having a DVB content of about 4 mol%.

elastic backbone and several polystyrene side chains, and a corresponding silylated ethylene/1-octene/DVB terpolymer. Fig. 10 (bottom) shows the complete disappearance of all vinyl peaks and a strong peak at 0.05 ppm corresponding to the methyl proton next to Si. Both the metallation and silylation efficiencies were almost 100%. Fig. 10 (top) indicates the graft copolymer containing more than 50 mol% polystyrene side chains. In addition to the chemical shifts for ethylene/1-octene, the new peaks ($\delta =$ 6.4–7.3 ppm) are due to aromatic protons in the PS side chains. Overall, the graft-from reactions were very effective — more than 80% styrene monomer conversion within one hour.

The graft content increased proportionally with increasing monomer concentration and reaction time. Since the graft-from reaction involves a living anionic polymerization, it is reasonable to assume that each benzylic lithium produces one polymer side chain and the each side chain has a similar molecular weight. The graft density, defined, as the number of grafted side chains per 1000 carbons in the polyolefin backbone, is the same as the density of the benzylic anions. The side chain length is basically proportional to the reaction time and monomer concentration.

In metallocene graft-onto reaction cases, the pending styrene units in the α-olefin/DVB copolymer serve as chain transfer agents. As discussed in Section 6.2, the combination of styrene and hydrogen is a very effective chain transfer agent in metallocene-mediated α-olefin polymerization, which can be directly applied to the graft reaction of an olefin/DVB copolymer containing pending styrene units, as illustrated in Eq. (10).

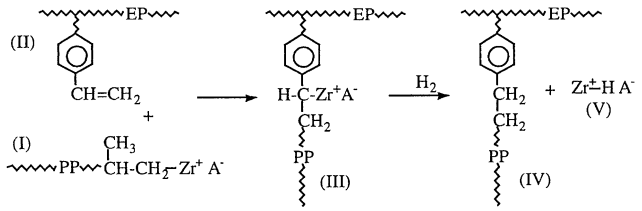

(10)

The metallocene polymerization of propylene was carried out in the presence of EP/DVB and hydrogen. During the polymerization of propylene (with a 1,2-insertion manner) the propagation Zr–C site (I) reacts with the pending styrene unit (with a 2,1-insertion manner) in the EP/DVB copolymer to form a graft copolymer (III) having several styrene terminated PP side chains. The catalytic Zr–C site in the graft copolymer (III) becomes inactive to propylene [47] due to the combination of steric hindrance between the active site (Zr–C) and the incoming monomer (propylene with 1,2-insertion), and the formation of a complex between the adjacent phenyl group and the Zr^+ ion. On the other hand, with the presence of hydrogen, the dormant Zr–C site (III) can react with hydrogen to form EP-*g*-PP (IV) and regenerate a Zr–H species (V) that is capable of reinitiating the polymerization of propylene and continuing the polymerization/graft reaction cycle. This process not only produces a desirable EP-*g*-PP graft polymer, but also maintains high metallocene catalyst activity. The PP's molecular weight is basically proportional to the [propylene]/[styrene] ratio.

Table 12 summarizes the results of EP-*g*-PP graft copolymers using a rac-Me_2Si[2-Me-4-Ph(Ind)]$_2ZrCl_2$/

Table 12
A summary of EP-*g*-PP graft copolymers

Reaction condition		Yield (g)	Catalyst activity Kg PP/molZr.h	Graft composition		Graft copolymer	
C_3/EP-DVB[a] (psi/g)	H_2 (psi)			EP-DVB (wt%)	PP (wt%)	T_g (°C)	T_m (°C)
20/2.6	0	2.5	0	100	0	−48	–
20/2.6	2	4.9	1864	32.3	67.7	−47	152
20/2.6	6	6.56	3184	30.5	69.5	−47	152
20/2.6	12	7.79	4128	28.5	71.5	−46	152

[a] EP-DVB: E: 52.1 mol%; P: 43.7 mol% and DVB: 4.2 mol%; $M_w = 68,600$ and PDI = 2.

MAO catalyst with the presence of propylene and EP-DVB and hydrogen. This systematic study was conducted to evaluate the effect of hydrogen on the catalyst activity and graft copolymer composition. The presence of hydrogen is clearly a key factor in the success of this graft reaction. With an appropriate [propylene]/[hydrogen] ratio, the graft reaction can be as efficient as the homopolymerization of propylene itself. The graft length and density can be controlled by the combination of DVB units in the EP-DVB copolymer and the propylene concentration. Some very desirable EP-*g*-PP graft copolymers containing continuous PP domains and discrete EP domains have been prepared with high impact TPO properties.

7.4. Ring-opening graft-from polymerization [67]

Ring opening polymerization provides a convenient route for preparing polyolefin graft copolymer containing polycondensation polymer side chains. Since the functionalized polyolefins are available, it is possible to use the functional group as an initiator for ring opening reactions. One example is an anionic ring opening reaction of ϵ-caprolactone (ϵ-CL) from a hydroxylated PP (PP-OH). In a typical example, a fine powder form of PP-OH ($M_v = 183,000$ g/mol), containing 1.4 mol% hexenol units is metallated with excess *n*-butyllithium to form the lithium alkoxide. A toluene slurry of the powdery solid was then reacted with a 3 molar equivalent of diethylaluminum chloride for 12 h to form the PP-aluminum alkoxide. The monomer, e.g. caprolactone, was then added to a slurry of the PP-O$AlEt_2$ in toluene. The reaction was terminated (after 24 h at room temperature) by the addition of MeOH, and the polymer was isolated via precipitation into acidified MeOH. The polymer mass was extracted with hot acetone in a soxhelet apparatus under N_2 for 48 h to remove any ϵ-CL homopolymer. The resulting PP-*g*-PCL graft copolymers were analyzed by NMR and DSC to determined their compositions and thermal properties (T_m, T_g, and crystallinity). Table 13 summarizes the experimental results of PP-*g*-PCL copolymers that were prepared from two PP-OH containing primary and secondary OH groups.

Runs 1–4 all started with the same PP-OH copolymer containing 1.4% hexenol monomer units. The weight percent PCL in the resulting graft copolymer increased linearly with increasing ϵ-CL in the feed. The relatively long reaction time can be explained by the heterogeneous reaction conditions. The diffusion of ϵ-CL into the PP matrix would be the rate limiting step for the reaction. In fact, runs 2 and 4 differ in the reaction time of 24 and 60 h, but resulted in copolymers with 33 and 59 wt% PCL respectively. The amount of homo-PCL produced, i.e. the acetone soluble fraction, also increased with the ϵ-CL feed. Any residual aluminum alkyl not covalently bound to the polymer could easily initiate the

Table 13
A Summary of PP-*g*-PCL copolymers and reaction conditions (Reproduced with permission from Macromolecules 1994;27:1313. Copyright 1994 Am. Chem. Soc.) [67]

Run	Reaction conditions			Products		
	PP-O-$AlEt_2$ (g)	ϵ-CL (g)	Time (h)	Acetone soluble (g)	Acetone insoluble (g)	ϵ-Cl in graft (wt%)
1	2	2.169	24	0.366	2.252	16.8
2	2	4.299	24	0.430	2.763	32.9
3	2	8.243	24	2.581	3.922	56.8
4	2	4.571	60	2.102	4.120	59.5
5	2	6.525	24	1.387	3.603	45.4

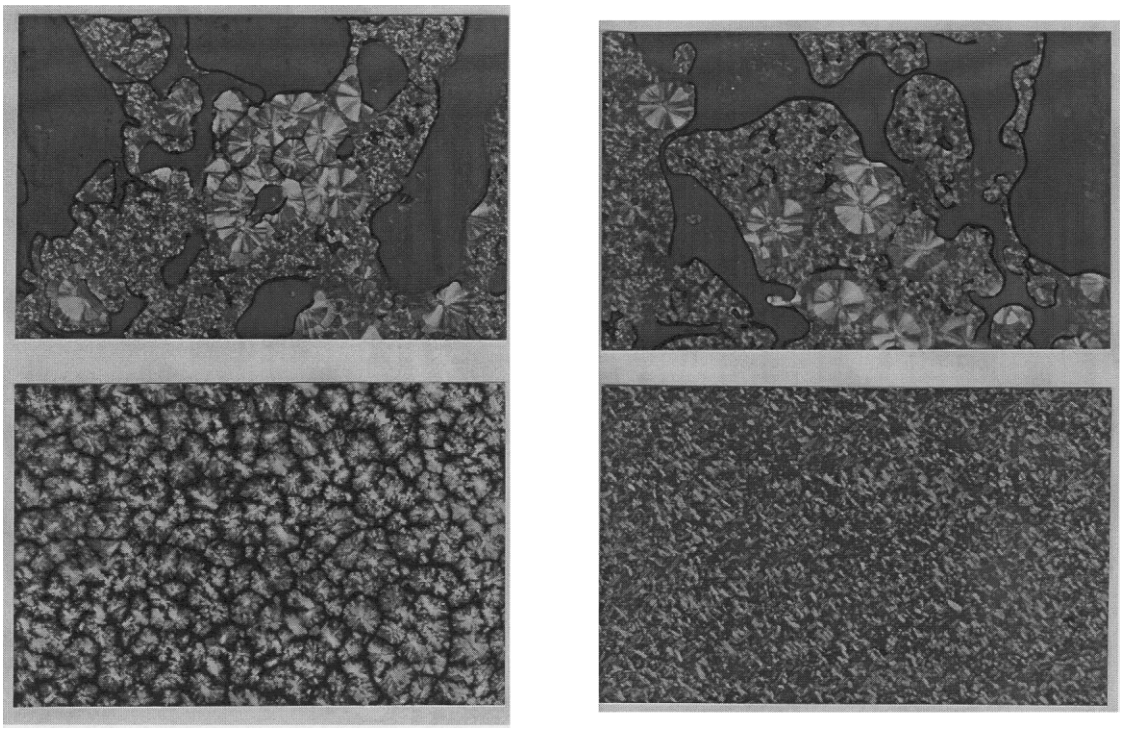

Fig. 11. Left: optical micrographs of (top) homopolymer blend with *i*-PP/PMMA = 70/30 and (bottom) two homopolymers with PP-*g*-PMMA containing 30% MMA, *i*-PP/PP-*g*-PMMA/PMMA = 70/10/30. Right: optical micrographs of (top) two homopolymer blend with *i*-PP/PC = 70/30 and (bottom) two homopolymers with PP-*g*-PCL, *i*-PP/PP-*g*-PCL/PC = 70/10/30 (100×). (Reproduced with permission from Macromolecules 1994;27:1313. Copyright 1994 Am. Chem. Soc.).

homo-polymerization of the ϵ-CL. Excess aluminum alkyl associated with the bound Al-Os may not be completely washed out by the non-polar solvents. Run 5 started with commercial grade propylene and 1,4-hexadiene copolymer containing approximately 1.6% unsaturated monomer units. The polymer was hydroborated with 9-BBN and oxidized to give functionalized PP with the secondary alcohols on either the 4 or 5 position of the hexadiene branch. The secondary alcohol can also be converted to the secondary aluminum alkoxide, which is recognized as an active initiator in the graft-from reaction of ϵ-CL.

7.5. Polyolefin graft copolymer as the compatibilizer in polyolefin blends

Polyolefin graft copolymers are very effective compatibilizers for improving interactions between their corresponding polyolefins and other materials, including polymers and substrates. Fig. 11 compares polarized optical microscopy of two polymer blend systems, including PP/PMMA [66] and PP/PC [67] with and without graft copolymers as the compatibilizers.

In the first system, a simple polymer blend (70/30 wt% of *i*-PP and PMMA homopolymers) shows two distinct phases — the crystalline PP phase and an amorphous PMMA phase. Within the PP domain, the spherulite size varies greatly with a few extremely large crystallites and predominantly small spherulites. With 10 wt% of PP-*g*-PMMA graft copolymer in PP/PMMA blend, the large phase seperated PMMA domains are dispersed into the inter-spherulite regions, and cannot be detected with the optical microscope.

The mode of nucleation within the PP crystalline phase has changed, as evidenced by the now relatively homogeneous spherulite size.

Bisphenol-A polycarbonate (PC) has excellent high and low temperature physical properties even up to 140°C. Using PP as the matrix material with a compatibilized polycarbonate dispersed phase could greatly improve the mechanical properties, creating a toughened plastic. Such an inexpensive polymer blend may be able to compete with more costly engineering plastics. Since poly(ϵ-caprolactone) (PCL) and polycarbonate (PC) form a miscible blend, the graft copolymer PP-*g*-PCL should behave as an emulsifier for PP and PC blends. In Fig. 14 (right), the 70/30 PP/PC blend shows gross phase separation of the spherulitic PP and the amorphous PC phases. The PC phases vary widely in both size and shape due to the lack of interaction with the PP matrix. On the other hand, the blend containing 70/30/10 of PP/ PC/ PP-*g*-PCL, where the graft contains 57 wt% PCL, shows only small distorted spherulites and a few very small distinct PC phases. The PP-*g*-PCL is clearly proven to be an effective compatibilizer for PP and PC blends. It should also be noted that the films of the compatibilized blends formed in the melt press were optically clear. This is unlike pure *i*-PP that forms hazy, translucent films. The lack of large spherulites in both the blend and the graft must minimize scattering.

It is interesting to study the compatibility of PE-*g*-PS copolymer in HDPE and PS blends. Both a polarized optical microscope and a scanning electron microscope (SEM) were used to examine the surfaces and bulk morphologies, respectively. Of the two blends comprised of an overall 50/50 weight ratio of PE and PS, one is a simple mixture of 50/50 between HDPE and PS and the other is a 45/45/10 weight ratio of HDPE, PS, and PE-*g*-PS (containing 50 mol% PS). Similar to Fig. 11, the polarized optical micrographs of the two blends are very different. A gross phase separation, with spherulitic PE and amorphous PS phases, is shown in the simple PE/PS blend. The PS phases vary widely in both size and shape due to the lack of interaction with the PE matrix. On the other hand, a continuous crystalline phase results in the compatibilized blend. Basically, the large phase separated PS domains are now dispersed into the inter-spherulite regions and cannot be detected by the optical microscope. The graft copolymer behaves as a polymeric emulsifier, and increases the interfacial interaction between the PE crystalline and the PS amorphous regions to reduce the domain sizes.

Fig. 12 shows the SEM micrographs, operating with secondary electron imaging, revealing the surface topography of the cold fractured film edges. The films were cryro-fractured in liquid N_2 to obtain an undistorted view representative of the bulk material. In the homopolymer blend, the polymers are grossly phase separated, as can be seen in Fig. 12(a). The PS component exhibits non-uniform, poorly dispersed domains and voids at the fracture surface. This 'ball and socket' topography is indicative of poor interfacial adhesion between the PE and PS domains, and represents PS domains that are pulled out of the PE matrix. Such pull out indicates that limited stress transfer takes place between the phases during fracture. A similar blend containing graft copolymer shows a totally different morphology in Fig. 12(b). The material exhibits flat mesa-like regions similar to pure PE. No distinct PS phases are observable, indicating that fracture occurred through both phases or that the PS phase domains are too small to be observed. The PE-*g*-PS is clearly proven to be an effective compatibilizer in PE/PS blends.

8. Synthesis of functional polyolefin diblock copolymers

Diblock copolymer is the most effective interfacial agent [73,74] in polymer blends and composites. Usually, only a small quantity (as low as 1%) of a suitable diblock copolymer is needed to change the

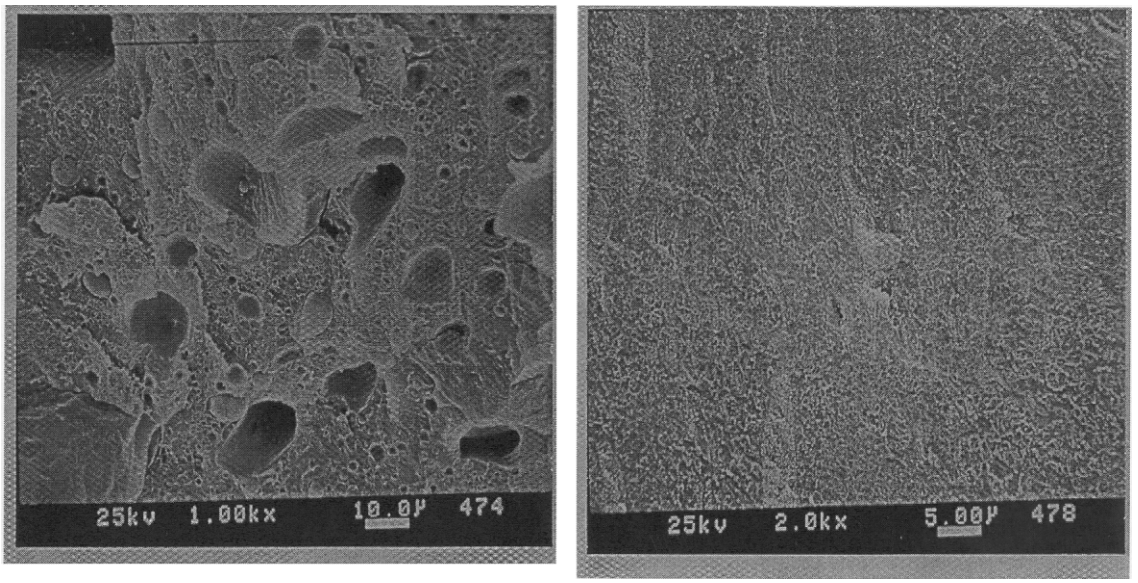

Fig. 12. SEM micrographs of the cross-section of two polymer blends: (a) two homopolymers with PE/PS = 50/50 (1000 ×) and (b) two homopolymers and a PE-*g*-PS copolymer blend with PE/PE-*g*-PS/PS = 45/10/45 (2000 ×) (Reproduced with permission from Macromolecules 1997;30:1272. Copyright 1997 Am. Chem. Soc.) [72].

incompatible binary blends to a uniform micro-phase morphology with strong interfacial adhesion.Traditionally, most diblock copolymers have been prepared by living polymerization processes, namely anionic [75,76], cationic [77,78], and recently metathesis [79,80] with sequential monomer additions. The living coordination polymerization of α-olefin by transition metals is very limited. In addition, the catalyst's sensitivity to functional groups further constrains the chemistry's ability in achieving functional polyolefin diblock copolymer.

In this section, we will discuss a new method by using polyolefin containing a terminal borane or *p*-MS groups, which can be interconverted to living free radical or anionic initiator, respectively, for polymerization of functional monomers. The chemistry employs two different polymerization mechanisms that are the most suitable for preparing individual polymer blocks, i.e. metallocene for polyolefin and free radical or anionic for functional polymer. The combination of two routes produces functional polyolefin diblock copolymers with a broad range of copolymer composition and well-designed molecular structure.

8.1. Polyolefin block copolymers prepared via a terminal borane group [50,51,81–83]

As illustrated in Eq. (11), polyolefin containing a terminal borane group (alkyl-9-BBN) can be prepared by two routes, i.e. in situ chain transfer reaction to B–H group during metallocene polymerization and hydroboration of chain-end unsaturated polymer (see details in Section 6.1). The terminal alkyl-9-BBN group in polymer (I) was then spontaneously oxidized to produce a peroxy-9-BBN (II). The peroxyborane (II) behaves very differently from regular organic peroxides, and consequently decomposes by itself even at ambient temperature to generate an alkoxy radical (C–O ∗) and a borinate radical (B–O ∗). The alkoxyl radical (C–O ∗), located at the end of polyolefin chain, is very reactive and can then be used for the initiation of radical polymerization with the presence of free radical

polymerizable monomers. On the other hand, the borinate radical (B–O ∗), stabilized by the empty p-orbital of boron through back-donating electron density, is too stable to initiate polymerization. However, the borinate radical may form a weak and reversible bond with the growing chain end during the polymerization reaction. Upon the dissociation of the electron pairs in the resting state, the growing chain end can then react with monomers to extend the polymer chain to form diblock copolymer (IV).

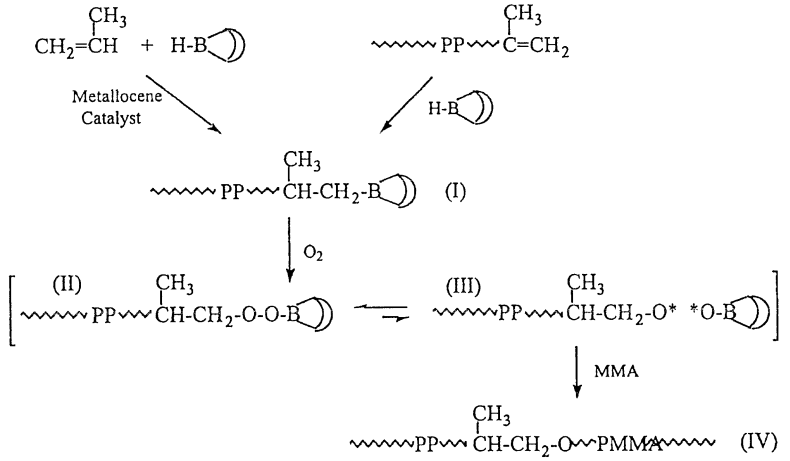

(11)

Overall, the reaction process resembles a transformation reaction from metallocene coordination polymerization to living free radical polymerization via a borane group at the polymer chain end. It is interesting to note that the reaction involves only one borane group per polymer chain. The whole reaction process provides an ultimate test for examining the efficiency of the borane reagent in the chain extension process.

One example is a borane-terminated PE (PE-*t*-B) polymer [50] that was subjected to oxidation reaction by oxygen in the presence of free radical polymerizable MMA monomers. The resulting reaction mixture was carefully fractionated by Soxlet extraction using boiling THF to remove any PMMA homopolymer. In most cases, only a very small amount (<10%) of PMMA homopolymer may be initiated by the radical in a bicyclic ring, instead of a polymeric radical, due to the small non-selective oxidation reaction of alkyl-9-BBN. The generally insoluble fraction (but soluble in 1,1,2,2-tetrachloroethane, 1,2,4-trichlorobenzene at elevated temperatures) is PE-*b*-PMMA diblock copolymer. Table 14 summarizes the experimental results of two sets of chain extension reactions using two starting PE-*t*-B polymers with $M_n = 19.4 \times 10^3$ and 42.7×10^3 g/mol, respectively.

The experimental result in both comparative sets clearly shows the increase of MMA conversion and the content of PMMA in the diblock copolymer with the increase of the reaction time. The extent of chain extension reaction is basically proportional to the reaction time, which clearly indicates the living free radical polymerization of MMA. High concentration of PMMA in diblock copolymer can be achieved with narrow molecular weight distribution.

Fig. 13 shows the ^{1}H NMR spectrum of three PE-*b*-PMMA copolymers that were sampled at different reaction times during the same chain extension process. The reaction was started by using a PE-*t*-B polymer (I) with $M_n = 19,400$ g/mol and $M_w/M_n = 2.1$. The new peak at 3.58 ppm, corresponding to methoxyl groups (CH_3O) in PMMA, increased its intensity with the reaction time. Apparently, the PMMA segment in PE-*b*-PMMA grows with the reaction time, and high molecular weight

Table 14
A summary of PE-*b*-PMMA diblock copolymers

	Reaction condition			THF extraction		Diblock copolymer		
PE-*t*-B[a] (g)	Temperature/time (°C/h)	O_2/MMA (ml/mol)	Yield (g)	Insoluble (%)	Soluble (%)	M_n ($\times 10^{-3}$)	M_w/M_n	PE/PMMA mole ratio
(I)/3	25/6	1.9/1.87	3.98	96	4	49.2	2.1	100:43
(I)/3	25/12	1.9/1.87	6.65	93	7	62.5	2.4	100:62
(I)/3	25/24	1.9/1.87	8.05	90	10	90.3	2	100:102
(II)/5	25/2	1.4/1.87	6.12	97	3	47.5	2.3	100:03
(II)/5	25/6	1.4/1.87	6.78	95	5	61.8	2.4	100:13
(II)/5	25/12	1.4/1.87	8.74	93	7	76.3	1.9	100:22
(II)/5	25/24	1.4/1.87	10.24	89	11	97.6	2.9	100:36

[a] PE-*t*-B (I): $M_n = 19.4 \times 10^3$ g/mol, $M_w/M_n = 2.1$; PE-*t*-B (II): $M_n = 42.7 \times 10^3$ g/mol; $M_w/M_n = 2.2$.

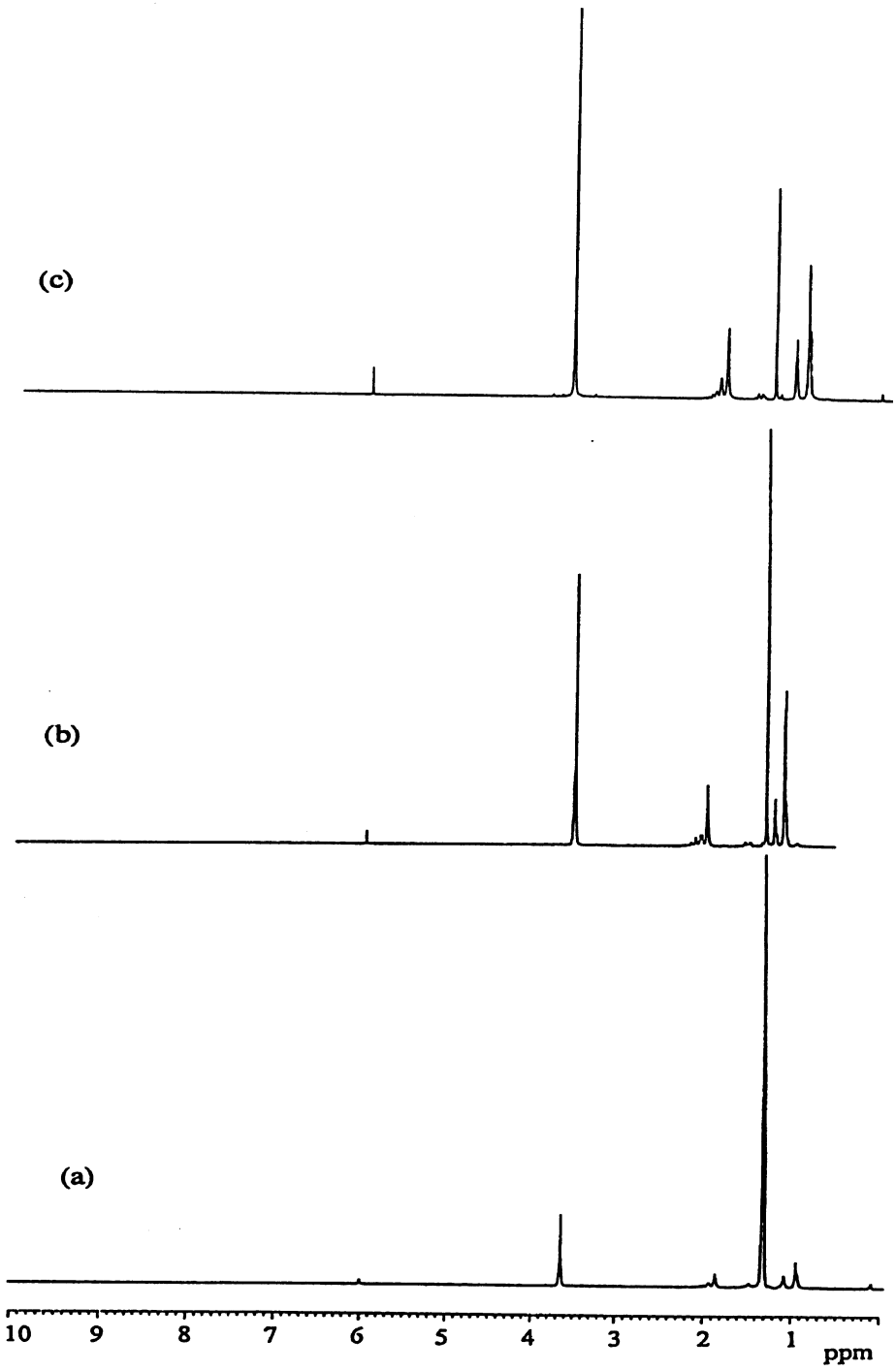

Fig. 13. ^{1}H NMR spectra of PE-*b*-PMMA containing (a) 16, (b) 48 and (c) 85 mol% PMMA contents. (solvent: $C_2D_2Cl_4$; temperature: 110°C).

diblock copolymer with up to 85 mol% of PMMA copolymer (Fig. 13(c)) has been prepared. Considering only one terminal borane group in each PE chain, these experimental results imply the living free radical polymerization in the chain extension process.

Fig. 14 compares the GPC curves of two PE-*b*-PMMA diblock copolymers and the starting PE-*t*-B polymer. It is clear that the polymer continuously increased its molecular weight during the entire polymerization process. The polymer's molecular weight distribution was maintained very constant and narrow ($M_w/M_n = 2.0$–2.2). The inset shows the linear plot of polymer molecular weight vs. the monomer conversion and compares the results with a theoretical line based on the [g of monomer consumed]/[mole of initiator]. A good match with the straight line through the origin strongly supports the presence of living polymerization in the reaction.

The same experimental results were observed in PP case [81], shown in Fig. 15. The molecular weight more than doubles from $M_n = 13,000$ of PP-*t*-B to $M_n = 29,000$ g/mol of PP-*b*-PMMA, and the molecular weight distribution (MWD) slightly increases from 1.5 to 1.7. The GPC results are consistent with the ^{1}H NMR measurements that show about a 1/1 mole ratio between PP and PMMA in the copolymer. It is very interesting to note the remarkable efficiency of borane terminal group, with only one unit per polymer chain.

The same radical chain extension was also applied to new syndiotactic–polystyrene (s-PS) [51]. Table 15 summarizes the reaction conditions and experimental results of *s*-PS diblock copolymers containing polymethylmethacrylate (PMMA) and polybutylmethacrylate (PBMA).

In general, both PMMA and PBMA blocks increase along with the reaction time, and chain extension reactions continue even after 12 h. Diblock copolymers with a nearly 1/1 mole ratio of [styrene]/[MMA] or [styrene]/[BMA] have been prepared, despite the heterogeneous reaction conditions. These effective

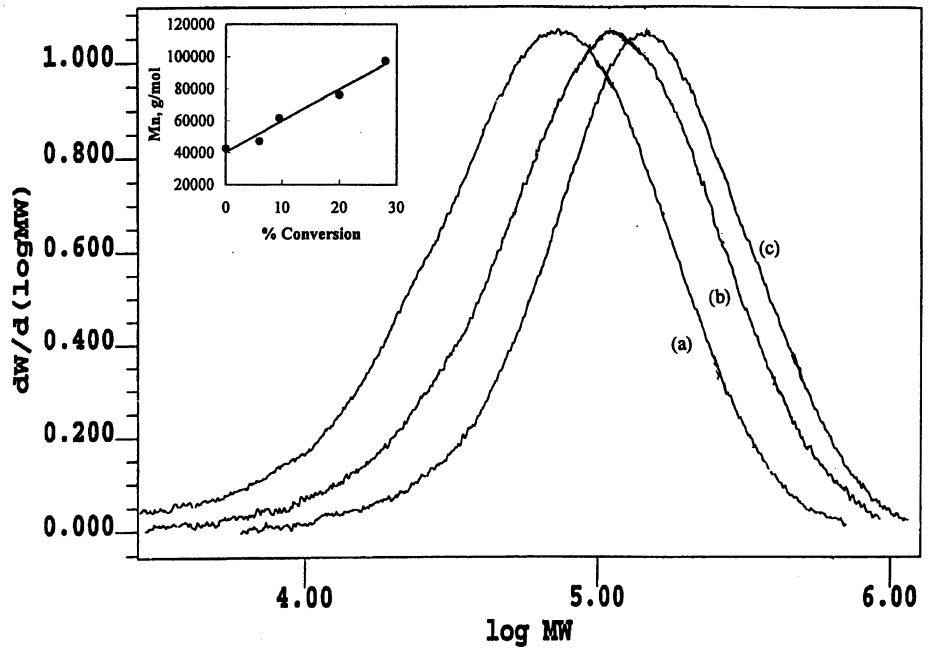

Fig. 14. GPC curves of (a) the starting PE-*t*-B polymer ($M_n = 19,400$), and two corresponding PE-*b*-PMMA copolymers (b) $M_n = 58,600$, and (c) $M_n = 90,300$ g/mol.

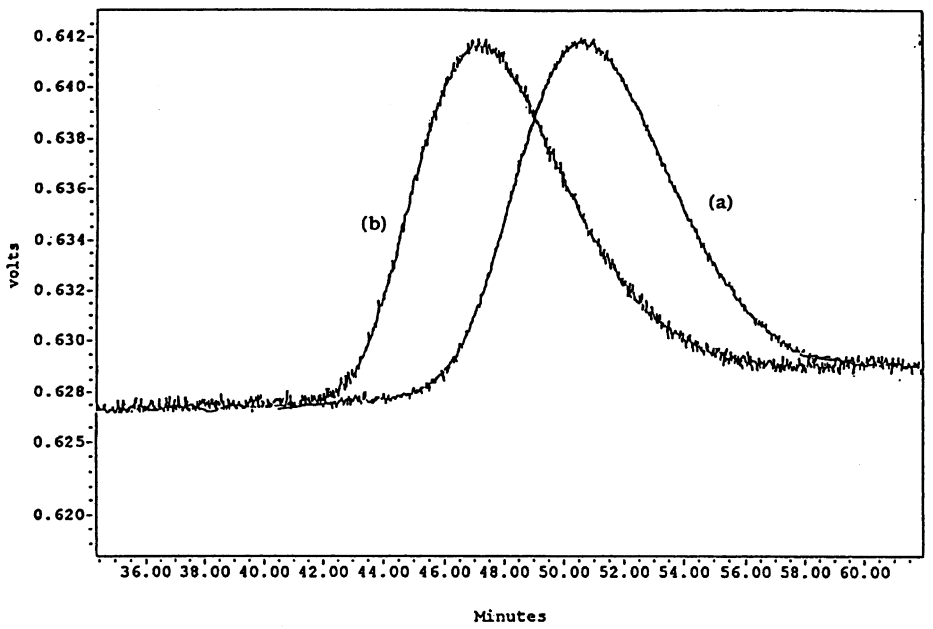

Fig. 15. GPC curves of (a) PP (M_n = 13,000 and PDI = 1.5) (b) the corresponding PP-*b*-PMMA copolymer (M_n = 29,000 and PDI = 1.7). (solvent: trichlorobenzene; temperature: 135°C). (Reproduced with permission from J. Am. Chem. Soc. 1999;121:6763. Copyright 1999 Am. Chem. Soc.).

and long-lived chain extension reactions again provide strong evidence of the borane group's existence at the polymer chain end and the living free radical chain extension process. DSC curves of *s*-PS-*t*-B and the corresponding *s*-PS-*b*-PMMA show two identical thermal transition temperatures, including a T_m near 270°C and a T_g near 100°C for the *s*-PS polymer, in both samples. A clear new T_g at about 130°C (corresponding to the high molecular weight PMMA polymer) was shown in *s*-PS-*b*-PMMA sample. Both polymer segments in the *s*-PS-*b*-PMMA copolymer must have long consecutive (undisturbed) sequences to form separate domains.

It's very interesting to note that the borane-mediated radical polymerization is particularly effective with the polar monomers. The rate of propagation may enhance due to the interaction between the boron moiety in the propagating end group and the heteroatom (O, N, Cl) in the polar monomer as illustrated below.

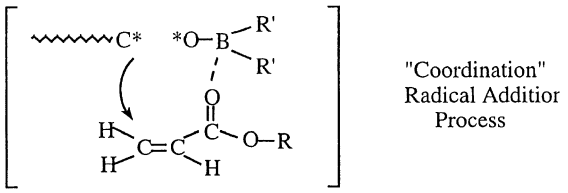

8.2. Polyolefin block copolymers prepared via a p-methylstyrene terminal group [52]

As discussed in Section 6.2, *p*-methylstyrene (*p*-MS) terminated polyolefins have been prepared by the combination of metallocene catalysis and chain transfer reaction to *p*-MS/H_2. The terminal *p*-MS

Table 15
A summary of *s*-PS-*b*-PMMA and *s*-PS-*b*-PBMA diblock copolymers

s-PS-*t*-B[a] (g)	Reaction condition		Polar monomer (mol)	Yield (g)	Diblock copolymer		Blocks mole ratio
	Temperature/time (°C/h)	O_2 (ml)			s-PS block M_n ($\times 10^{-3}$)	Polar Block M_n ($\times 10^{-3}$)	
(I)/5	25/6	1.9	MMA/1.87	6.25	15	2	100:14
(I)/5	25/12	1.9	MMA/1.87	7.56	15	5	100:35
(I)/5	25/24	1.9	MMA/1.87	9.98	15	14	100:97
(I)/5	25/10	1.9	BMA/1.87	6.72	15	7.1	100:35
(I)/5	25/20	1.9	BMA/1.87	7.56	15	15	100:72
(I)/5	25/24	1.9	BMA/1.87	8.94	15	18.3	100:89
(II)/7	25/6	2.4	MMA/1.87	7.56	70	3	40:04.5
(II)/7	25-Dec	2.4	MMA/1.87	8.13	70	8	100:12
(II)/7	25/24	2.4	MMA/1.87	8.98	70	17	100:25

[a] s-PS-*t*-B (I): $M_n = 15 \times 10^3$ g/mol, $M_w/M_n = 2.2$; *s*-PS-*t*-B (II): $M_n = 70 \times 10^3$ g/mol; $M_w/M_n = 2.1$.

Table 16
A summary of PP-*b*-PS diblock copolymers

Reaction conditions			Yield (g)	PP-*b*-PS products		M_n (g/mol)	M_w/M_n
PP[a] (g)	Styrene (g)	Time (h)		THF soluble (g)	PP-*b*-PS products, PP/PS (mol)		
0.73	0.9	1.0	0.94	n.g	86.9/13.1	–	–
0.73	2.7	1.0	1.54	n.g	60.6/34.4	54.0	2.34
0.69	4.5	3.0	2.77	n.g	52.2/47.8	–	–
0.76	9.0	3.0	3.60	n.g	48.8/51.2	117.5	2.25

[a] PP-*t*-*p*-MS sample ($M_n = 25.9 \times 10^3$ g/mol; $M_w/M_n = 2.3$).

group provides the active site to transform metallocene polymerization to living anionic polymerization, as illustrated in Eq. (12). The metallation reaction of *p*-MS terminated polypropylene (PP-*p*-MS) was carried out under heterogeneous reaction conditions by suspending the powder form of PP in cyclohexane. A excess of *s*-BuLi/TMEDA was used to ensure a complete reaction. Usually, the reaction mixture was stirred at room temperature for a few hours before removing the polymer powder from the solution by filtration and washing. The lithiated PP-*t*-*p*-MS (II) was used to prepare diblock copolymers. By mixing polymer powder with styrene monomer in cyclohexane solvent, the living anionic polymerization took place to produce PP-*b*-PS diblock copolymer. After the reaction, the product was vigorously extracted by refluxing THF to remove any PS homopolymer.

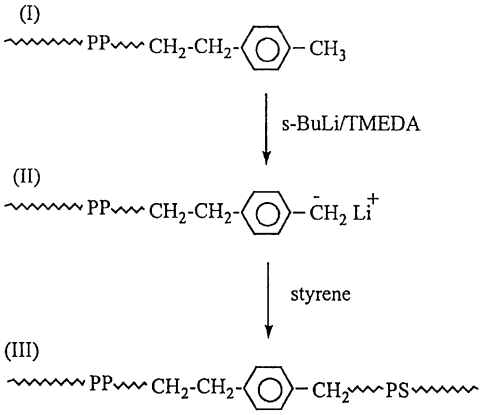

(12)

Table 16 summarizes the experimental results of PP-*b*-PMMA diblock copolymers by starting from a PP-*t*-*p*-MS polymer ($M_n = 25.9 \times 10^3$ g/mol). In all cases (including high molecular weight PP-*t*-*p*-MS polymer cases), the soluble PS homopolymer fraction was negligible. Basically, the PP-*b*-PS product increases its PS content and molecular weight as more styrene is introduced during the reaction. Not all of the styrene was converted in the relatively short reaction time under non-polar solvent conditions.

Fig. 16 (top) shows the ^{1}H NMR spectra of PP-*b*-PS ($M_n = 44.0 \times 10^3$ g/mol; PDI = 2.34) and Fig. 16 (bottom) compares the GPC curve of PP-*b*-PS with the starting PP-*t*-*p*-MS ($M_n = 25.9 \times 10^3$ g/mol; PDI = 2.3). Despite the doubling of polymer molecular weight, the molecular weight distribution (PDI) remains very constant. The quantitative analysis of the diblock copolymer composition was calculated

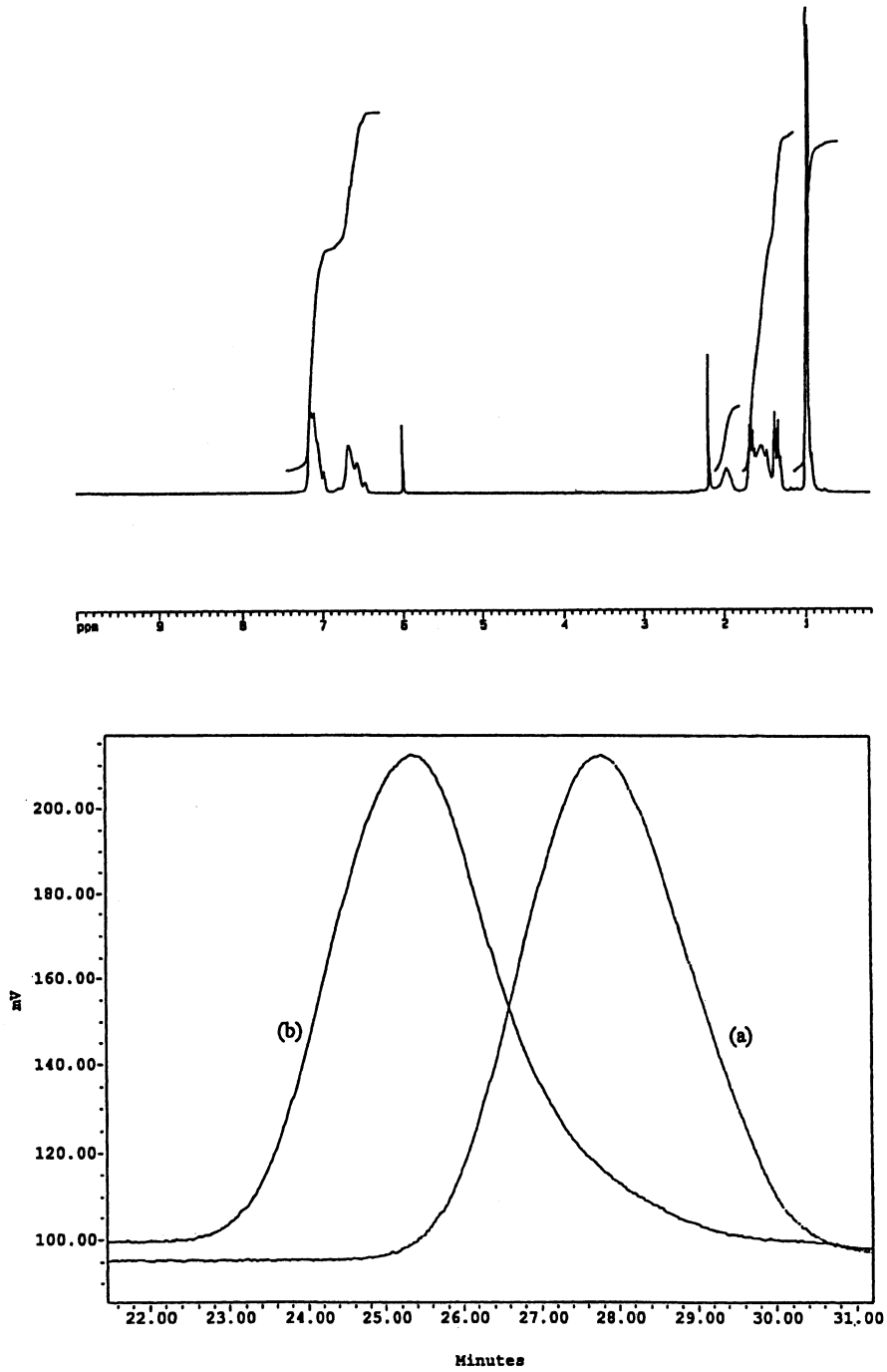

Fig. 16. Top: ^{1}H NMR spectra of PP-*b*-PS diblock copolymer and (bottom) GPC curves of (a) the starting PP-*t*-*p*-MS and (b) the resulting PP-*b*-PS polymers. (Reproduced with permission from J. Am. Chem. Soc. 2001;123:4871. Copyright 2001 Am. Chem. Soc.).

using the ratio of two integrated intensities between the aromatic protons ($\delta = 6.4$–7.3 ppm) in the PS segment and the methylene protons ($\delta = 1.35$–1.55 ppm) in the PP segment, along with the number of protons both chemical shifts represent.

Overall, the transformation from metallocene to living anionic polymerization was very effective (>80%), and the molecular structure of the copolymer could be easily controlled by the starting *p*-MS terminated polyolefin and the quantity of monomer introduced during the living anionic chain extension reaction. This diblock reaction benefits from the known and well-defined living anionic polymerization process, and offers a complementary method to the previous one, i.e. transformation from metallocene to living free radical polymerization. The combination provides a powerful tool to prepare a broad range of polyolefin diblock copolymers containing a metallocene-prepared polyolefin block and an anionic or free radical-prepared polymer block.

9. Conclusion

It is both a scientific challenge and an industrial importance to develop a general method of preparing functional polyolefin with block and graft structures, containing both polyolefin and functional (polar) polymer blocks. The reactive polyolefin intermediate offers a very attractive route, with simple reaction process to prepare the desirable block and graft copolymers with relatively well-defined molecular structures. The chemistry is based on three reactive sites, including borane, *p*-methylstyrene, and divinylbenzene, which permit the facile transformation from metallocene-mediated olefin polymerization to living free radical or living anionic polymerization. This sequential polymerization process, with both changes of catalytic sites and monomers, allows the employment of the best suitable polymerization mechanisms for preparing individual polymer blocks, i.e. metallocene polymerization for polyolefin and free radical or anionic polymerization for functional (polar) polymer.

Acknowledgements

The authors would like to thank the Office of Naval Research and the Petroleum Research Foundation for their financial support.

References

[1] Storck WJ. Chem Engng News 2000;78(26):9.
[2] Vasile C, Seymour RB. Handbook of polyolefins. New York: Marcel Dekker, 1993.
[3] VerStrate G. Enyclop Polym Sci Engng 1986;6:522.
[4] Perlson BD, Schababerle CC. In: Ehrig RJ, editor. Plastics recycling; products and process. Munich: Hanser Publishers, 1992. Chapter 4.
[5] Natta G, Mazzanti G, Longi P, Bernardini F. J Polym Sci 1958;31:181.
[6] Heller J, Tieszen DO, Parkinson J. J Polym Sci 1963;A1:125.
[7] Clark KJ, Powell T. Polymer 1965;6:531.
[8] Chung TC. Macromolecules 1988;21:865.
[9] Andresen A, Cordes HG, Herwig J, Kaminsky W, Merk A, Mottweiler R, Pein J, Sinn H, Vollmer HJ. Angew Chem, Int Ed Engl 1976;15:630.
[10] Sinn H, Kaminisky W. Adv Organomet Chem 1980;18:99.

[11] Ewen JA, Jones RL, Razavi A, Ferrara J. J Am Chem Soc 1988;110:6255.
[12] Yang X, Stern L, Marks TJ. J Am Chem Soc 1994;116:10015.
[13] Coates GW, Waymouth RM. Science 1995;267:217.
[14] Francis FC, Brookhart M. J Am Chem Soc 1995;117:1137.
[15] Mecking S, Johnson LK, Wang L, Brookhart M. J Am Chem Soc 1998;120:888.
[16] Clark KJ, City WG. US Patent 3,949,277, 1970.
[17] Langer AW, Haynes RR. US Patent 3,755, 279, 1973.
[18] Purgett MD, Vogl O. J Polym Sci, Part A: Polym Chem 1988;26:677.
[19] Kesti MR, Coates GW, Waymouth RM. J Am Chem Soc 1992;114:9679.
[20] Schneider MJ, Schafer R, Mulhaupt R. Polymer 1997;38:2455.
[21] Correia SG, Marques MM, Ascenso JR, Ribeiro AFG, Gomes PT, Dias AR, Blais M, Rausch MD, Chien JCW. J Polym Sci, Part A: Polym Chem 1999;37:2471.
[22] Gaylord NG, Mehta M, Mehta R. J Appl Polym Sci 1987;33:2549.
[23] Singh R. Prog Polym Sci 1992;17:251.
[24] Jagur-Grodzinski J. Prog Polym Sci 1992;17:361.
[25] Hu GH, Flat JJ, Lambla M. Free radical grafting of monomers onto polymers by reactive extrusion: principles and applications. In: Al-Malaika S, editor. Reactive modifiers for polymers. London: Blackie Academic and Professional, 1997. p. 1–77.
[26] Hogt AH, Meijer J, Jelenic J. Modification of polypropylene by organic peroxides. In: Al-Malaika S, editor. Reactive modifiers for polymers. London: Blackie Academic and Professional, 1997. p. 84–123.
[27] Chung TC. ChemTech 1991;27:496.
[28] Chung TC. J Mol Catal 1992;76:15.
[29] Chung TC. Macromol Symp 1995;89:151.
[30] Chung TC. Trends Polym Sci 1995;3:191.
[31] Chung TC. Polym Mater Encycl 1996;8:6412.
[32] Chung TC. Metallocene-based reactive polyolefin copolymers containing *p*-methylstyrene. In: Scheirs J, Kamisky W, editors. Metelocene-based polyolefins. New York: Wiley, 1999. p. 293–318.
[33] Aggarwal SL. Block copolymers. New York: Plenum Press, 1970.
[34] Riess G, Periard J, Bandereet A. Colloidal and morphological behavior of block and graft copolymers. New York: Plenum Press, 1971.
[35] Lohse D, Datta S, Kresge E. Macromolecules 1991;24:561.
[36] Chung TC. US Patent 4,734,472, 1989.
[37] Chung TC. US Patent 4,812,529, 1989.
[38] Ramakrishnan S, Berluche E, Chung TC. Macromolecules 1990;23:378.
[39] Chung TC, Lu HL, Li CL. Polym Int 1995;37:197.
[40] Chung TC, Rhubright D. Macromolecules 1991;24:970.
[41] Chung TC, Rhubright D. Macromolecules 1993;26:3019.
[42] Chung TC, Lu HL. US Patent 5,543,484, 1996.
[43] Chung TC, Lu HL. US Patent 5,866,659, 1999.
[44] Chung TC, Lu HL. US Patent 6,015,862, 2000.
[45] Chung TC, Lu HL. J Polym Sci Part A: Polym Chem 1997;35:575.
[46] Chung TC, Lu HL. J Polym Sci, Part A: Polym Chem 1998;36:1017.
[47] Lu HL, Hong S, Chung TC. J Polym Sci, Part A: Polym Chem 1999;37:2795.
[48] Lu HL, Hong S, Chung TC. Macromolecules 1998;31:2028.
[49] Chung TC, Dong JY. US Patent 6,096,849, 2000.
[50] Xu G, Chung TC. J Am Chem Soc 1999;121:6763.
[51] Xu G, Chung TC. Macromolecules 1999;32:8689.
[52] Chung TC, Dong JY. J Am Chem Soc 2001;123(21):4871.
[53] Chung TC, Lu HL, Li CL. Macromolecules 1994;27:7533.
[54] Chung TC, Rhubright D. J Polym Sci, Part A: Polym Chem 1993;31:2759.
[55] Machida S, Shikuma H, Tazaki T, Tatsumi T, Kurokawa S. US Patent 5,608,009, 1997.
[56] Doi Y, Ueki S, Soga K. Macromolecules 1979;12:814.

[57] Doi Y, Keii T. Adv Polym Sci 1986;73/74:201.
[58] Yasuda X, Furo M, Yamamoto H. Macromolecules 1992;25:5115.
[59] Killian CM, Tempel DJ, Johnson LK, Brookhard M. J Am Chem Soc 1996;118:11664.
[60] Baumann R, Davis WM, Schrock RR. J Am Chem Soc 1997;119:3830.
[61] Natta G, Beati E, Severine F. J Polym Sci 1959;34:548.
[62] Ranby B, Guo F. Polym Prepr 1990;31:446.
[63] Chung TC, Jiang GJ, Rhubright D. US Patent 5,286,800, 1994.
[64] Chung TC, Jiang GJ, Rhubright D. US Patent 5,401,805, 1995.
[65] Chung TC, Jiang GJ. Macromolecules 1992;25:4816.
[66] Chung TC, Rhubright D, Jiang GJ. Macromolecules 1993;26:3467.
[67] Chung TC, Rhubright D. Macromolecules 1994;27:1313.
[68] Chung TC, Janvikul W, Lu HL. J Am Chem Soc 1996;118:705.
[69] Chung TC, Janvikul W. J Organomet Chem 1999;581:176.
[70] Chung TC, Janvikul W, Bernard R, Jiang GJ. Macromolecules 1993;27:26.
[71] Chung TC, Janvikul W, Bernard R, Hu R, Li CL, Liu SL, Jiang GJ. Polymer 1995;36:3565.
[72] Chung TC, Lu HL, Ding RD. Macromolecules 1997;30:1272.
[73] Riess G, Periard J, Bonderet A. Colloidal and morphological behavior of block and graft copolymers. New York: Plenum Press, 1971.
[74] Lohse D, Datta D, Kresge E. Macromolecules 1991;24:561.
[75] Szwarc M. Adv Polym Sci 1982;47:1.
[76] Young RN, Quirk RP, Fetters L. J Adv Polym Sci 1984;56:1.
[77] Miyamoto M, Sawamoto M, Higashimura T. Macromolecules 1985;18:123.
[78] Kennedy JP. US Patent 4,946,899, 1990.
[79] Risse W, Grubbs RH. Macromolecules 1989;22:1558.
[80] Schrock RR, Yap KB, Yang DC, Sitzmann H, Sita LR, Bazan GC. Macromolecules 1989;22:3191.
[81] Chung TC, Lu HL, Janvikul W. Polymer 1997;38:1495.
[82] Chung TC, Lu HL. J Mol Cat A: Chem 1997;115:115.
[83] Lu B, Chung TC. Macromolecules 1999;32:2525.